Final Report – Phase II

# ENERGY EFFECTIVENESS OF ARRAYS OF WIND ENERGY CONVERSION SYSTEMS

Prepared for

National Swedish Board for Energy Source Development
Box 21048
S-11428 Stockholm, Sweden



By

Peter B.S. Lissaman and Edward R. Bate, Jr.

AeroVironment Inc.
145 Vista Avenue
Pasadena, California 91107
U.S.A.

May 1977

## ABSTRACT

A method of predicting power output of a general array of wind turbines is given. This involves a FORTRAN IV computer program capable of handling 100 identical wind turbine units at any power coefficient or height in an arbitrary geometrical array on level terrain. The ambient turbulence level of the natural wind is an important parameter in the analysis. The program gives total power flux available as the wind direction varies through $360^{o}$.

The fluid mechanics of wake development are analyzed and it is shown that the momentum deficit behind each unit will be conserved downstream. Thus, if radius and wake profile are known, the wake velocity can be determined. Wake profiles established from previous experimental work in co-flowing jets are used, and wake radius determined by assuming the wake growth is caused by both ambient and mechanically generated turbulence. The latter controls the initial growth, while ambient turbulence dominates the downstream development. A procedure to handle the combined effects of ambient and mechanical turbulence is given. Ground effect is simulated by standard imaging techniques, and multiple turbine interactions by averaging and superposition methods.

The fluid mechanics are based on work in a preceding report and are thus only briefly outlined here. The computer program is treated in detail with mathematical algorithms for all quantities and includes a listing of the program with flow charts and input instructions. Plots of power against wind direction are given for six arrays of increasing complexity.

Finally, suggestions for further work are made. These involve field testing to prove the basic assumptions, more elaborate fluid mechanics and meteorological analyses, and improved automation of program by the addition of ancillary subprograms.

ACKNOWLEDGEMENTS

The authors would like to express their very great appreciation of the work of Mr. Torgny Faxen, representative of the National Swedish Board for Energy Source Development, who had a major role in designing, programming, debugging and testing the computer codes. Mr. Faxen's diligence and enthusiasm contributed significantly to this research.

They would also like to express their appreciation to Mr. Sven Hugosson, of the above organization, whose competent and intelligent management of the program ensured that the scientific work proceeded expeditiously and effectively; and to Dr. Olle Ljungstrom, whose farsighted approach to wind energy created the initial ideas on which this work is based.

TABLE OF CONTENTS


| | | Page |
|---|---|---|
| | ABSTRACT | i |
| | ACKNOWLEDGEMENTS | ii |
| 1. | INTRODUCTION | 1-1 |
| 2. | DESCRIPTION OF COMPUTER MODEL | 2-1 |
| 2.1 | Outline of Concepts Used in Computer Model | 2-1 |
| 2.2 | Assumptions Used | 2-2 |
| 2.3 | Geometry of Wake Regions | 2-5 |
| 2.4 | Velocity Profiles | 2-10 |
| 2.5 | Addition of Velocities | 2-11 |
| 2.6 | Ground Plane | 2-13 |
| 2.7 | Integration of Power and Average Velocity across Receptor Disk | 2-13 |
| 2.8 | Array Geometry | 2-16 |
| 2.9 | Summation of Array Elements | 2-18 |
| 2.10 | Program Logic | 2-20 |
| 3. | FLUID MECHANICS | 3-1 |
| 3.1 | Wake Growth and Geometry | 3-1 |
| 3.2 | Interacting Wakes | 3-6 |
| 3.3 | Ground Plane | 3-8 |
| 3.4 | Initial Expansion Region | 3-8 |
| 3.5 | Transition Region Velocity Profile | 3-10 |
| 3.6 | Upstream Meteorology and Boundary Layer Effects | 3-12 |
| 3.7 | Relationship between m and $C_P$ | 3-13 |
| 4. | EXERCISE OF COMPUTER | 4-1 |
| 4.1 | General | 4-1 |
| 4.2 | Centerline Power Ratio for Simple Geometry | 4-1 |
| 4.3 | Complex Array Geometries | 4-4 |
| 5. | RECOMMENDATION FOR FURTHER WORK | 5-1 |
| 5.1 | General | 5-1 |
| 5.2 | Correlation with Test Results | 5-2 |
| 5.3 | Improved Fluid Mechanical Modeling | 5-2 |
| 5.4 | Improved Meteorological Modeling | 5-3 |
| 5.5 | Augmentation of the Computer Coding | 5-4 |
| 6. | REFERENCES | 6-1 |
| | APPENDIX – Determination of Effective Growth Rate in Region III | |

# 1. INTRODUCTION

Wind turbines are devices for extracting power from the wind energy flux in the planetary boundary layer, usually near the ground. The flow downstream of such energy extraction devices is markedly influenced by the energy extraction process. The resulting momentum deficit wakes behind the turbines contain flow of lower velocity than the upstream value and the performance of other machines located in the downstream portions of such wakes (as in an array of wind turbines, for instance) will be seriously affected by this slower flow.

Because of the many variables that are involved in the wake flow in a typical wind turbine array, the prediction of wake size, location, and velocity, and the effects of interactions between multiple wakes is a problem which is tractable only with the aid of the digital computer. Even then, some of the complicating influences of real fluid effects must be approximated or sometimes neglected in order to obtain a solution.

The present study has resulted in a computer code from which the effective power from an arbitrary array of wind turbines with arbitrary wind direction may be determined. The assumptions used to define the particular problem solved here are stated below.

An arbitrary array of wind turbines is situated on flat, level terrain. The wind entering the array is steady and has a uniform velocity profile. The wind may have any arbitrary direction; the wind turbines can weathercock so that their power extraction disks are always perpendicular to the wind. Thus, in wind-oriented coordinates, the geometry of the array varies with wind angle.

Each wind turbine in the array produces a wake which establishes a downstream velocity field of lower magnitude than free stream. The wakes from all the wind turbines are superimposed to determine the total velocity at any arbitrary location in the array. The wind turbines are all operated

such that the initial velocity decrement across each extraction disk is always a constant fraction of the oncoming flow (all machines operate at constant local power coefficient). This is the case whether the oncoming flow to a particular receptor disk is free stream velocity (as it would be for the wind turbines in the first row in an array) or the reduced wake velocity due to the presence of upstream wind turbines.

The growth of the momentum wake in the downstream direction is a result of the turbulent velocities produced by the mechanical turbulence from the wind turbine itself and the ambient turbulence, associated with the free stream flow. The mechanical term primarily influences initial wake growth. The latter stages of wake growth are primarily influenced by the ambient term which is a superimposed effect on wake growth whose magnitude is determined by the meteorological conditions upstream of the array.

The ground plane retards wake flow re-energization and has been acounted for in the present model by standard image techniques.

The power available to each wind turbine in the array is determined for that wind turbine as "receptor," with each of the other wind turbines as wake generators. In turn, each wind turbine plays the role of receptor. The power for the entire array is determined by summing over all the receptors and then determining the average.

In this manner, the relationship of total power available to the array as a function of wind angle is determined. This relationship represents a unique function for a given array and is helpful in determining optimum wind orientation. In addition, it may be utilized to predict array performance for non-optimum wind directions and it may be integrated to determine the effect of variable wind angles.

Further refinements to the computer model will result in refinements to this relationship between array power and wind direction predicted by the

model. Thus, variable profile oncoming winds (boundary layer flow), non-level terrain in the array, and operation of the individual wind turbines at variable $C_p$ will produce changes in the model output. However, the primary form of the relationship between array power and wind direction is determined by the array geometry and the manner in which the wind turbine wakes interact with each other and with the other wind turbines in the array. This is all accounted for in the present model and as such, the model represents a tool for the design of wind turbine arrays.

## 2. DESCRIPTION OF COMPUTER MODEL

### 2.1 Outline of Concepts used in Computer Model

The basic concepts used in developing the flow model have been analyzed in a previous report (Lissaman, 1977) and are further described in a later section. This section essentially displays the mathematical algorithms used in constructing the computer model. It is, however, helpful at this stage to discuss in general terms the concepts used in deriving these equations.

It is assumed that the non-dimensional profiles in the wake are those given by Abramovitch (1963) for the various regions. Thus if one knows the wake radius (or scale) the centerline velocity deficit can always be determined by invoking the principle that the momentum deficit is conserved. This momentum deficit can be directly related to the parameter m, the ratio of the outer flow velcoity to the inviscid slipstream velocity. Consequently, for any cross-section, the relationships given by Abramovitch between wake radius, centerline velocity and m all obtain identically in the present analysis. However, the growth rates determined by Abramovitch apply only for a non-turbulent outer flow. Consequently, in our analysis all these growth rates must be modified by incorporating the effect of ambient turbulence. Essentially this is done by assuming that the growth rates are additive in the following sense:

$$(dr/dx)_e^2 = (dr/dx)_a^2 + (dr/dx)_m^2$$

where the first term is the square of the effective growth rate and $(dr/dx)_a$, $(dr/dx)_m$ are growth rates due to ambient and mechanical turbulence respectively. Now $(dr/dx)_m$ can be determined from experimental results quoted by Abramovitch while $(dr/dx)_a$ is assumed constant for a given value of atmospheric turbulence. Thus, in each region modified effective growth rates can be rationally determined.

The construction of the computer algorithms now becomes clear. The velocity profile is of different form in different stages of growth, but this form is uniquely defined. Thus for each profile region, knowing the growth rate, the radius can be determined, then for a given velocity profile the centerline velocity is uniquely determined by the condition that momentum deficit is conserved.

In the following portions of this chapter the different wake regions are defined, and the characteristic growth rates specified. The equations and numerical constants appearing in the various relationship are taken directly from Abramovitch and apply in our case because we have assumed the Abramovitch profiles obtain.

## 2.2 Assumptions Used

The computer model directly treats the complicated interaction of wind turbine wakes in a multi-wind turbine array for all angles of the external wind. It calculates the power received by each wind turbine and then sums and find the average for the array as a whole.

The wake of a single unit is shown in Figure 2-1, as idealized for an unbounded flow. It is divided into four regions for the calculations. The wake radii in each of these regions increase linearly with downstream distance at rates set by the effective turbulence, which is a combination of the mechanical and ambient turbulence. The details of the geometry and flow in these regions will be discussed in the next two sections.

Region I extends to $X = X_H$, the point at which the shear due to the outer flow has completely eroded the potential core of uniform flow downstream of the extraction disk. Velocity profiles across the wake in this region are not self-similar at various downstream locations due to the change in relative size of the core flow and turbulent mixing zone. At the end of Region I a continuous shear layer-like velocity profile has completely developed but is represented by a slightly different functional form from

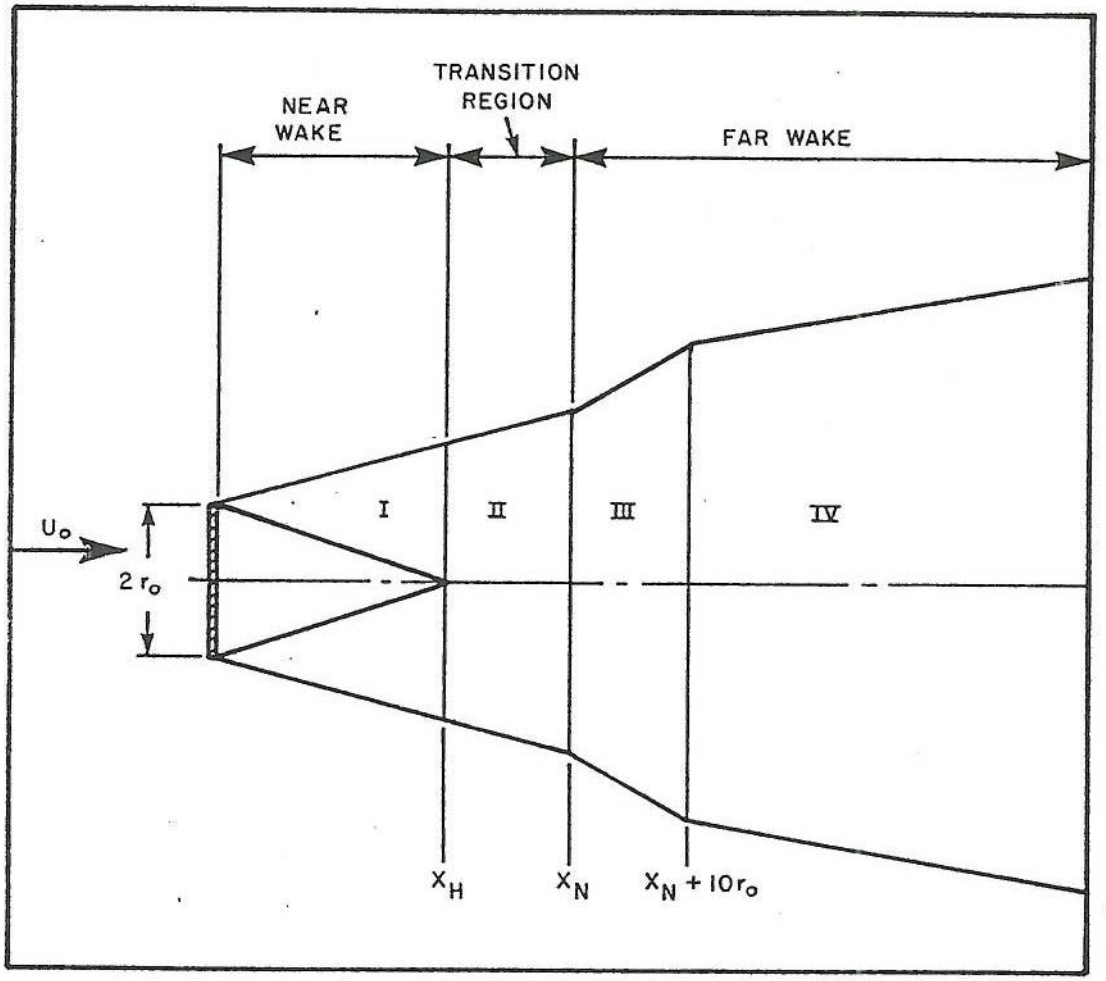


FIGURE 2-1. Wake geometry for computer model.

that used later in the far wake regime. The transition region, Region II, allows for the smooth transition of the completely developed near wake velocity profile to that used in the far wake, which is self-similar for all subsequent downstream locations.

Region I also includes the expansion of the wake from the diameter of the physical extraction disk, $r_d$, to the expanded slipstream value, $r_o$, that is the slipstream expansion due to potential effects. The computer model assumes that this expansion occurs at the station of the disk, itself so that the wake develops from $r = r_o$ at $x = 0$. Section 3.4 discusses the reasons for this assumption.

Wake growth rate is identical for regions I and II and is given by a combination of ambient and mechanical turbulence as discussed by Lissaman (1977). The end of region II occurs at $X_N = nX_H$, where n is a function of the mechanical turbulence as described by Abramovitch (1963). $X_H$ is related to the disappearance of the potential core, which is influenced by both the mechanical and ambient turbulence. The wake radius at the end of Region I is a function only of the total drag of the wind turbine and the assumed velocity profile there. The wake radius at the end of Region II can be found from the radius at the end of Region I and the values of $X_H$ and $X_N$.

Region III represents the region in the far wake where mechanical turbulence is decaying but where both mechanical and ambient turbulence influence wake growth. It is set at $\Delta X = 10r_o$ in length; by which distance ambient turbulence is dominant.

To determine the relative effect of these two turbulence mechanisms a series of numerical integrations were made. These are described fully in Lissaman (1977), and here we repeat the basic concept. At the start of the region the turbulence due to mechanical and ambient effects was combined, and a rate of radius growth determined and the new radius a short distance downstream determined. At this station the new centerline velocity was

determined by conserving momentum deficit, so that the new mechanical turbulence associated with this radius could be found. The ambient turbulence was combined with this mechanical turbulence and the process continued as a numerical integration. From the final wake radius the effective turbulent growth rate $\alpha_e$ could then be determined. It was found that for all values of ambient turbulence above $\alpha = 0.05$ the wake growth was very nearly linear, so that an effective linear growth rate $\alpha_e$ could be determined by dividing the change in radius by the length over which growth occurs. This rate is, of course, a function of the ambient term represented by $\alpha$ and the mechanical term represented by m. This calculation is outlined in the Appendix.

Figure 2-2 shows the resulting relationship between $\alpha_e$, $\alpha$, and m. $\alpha_e$ is used as an input to the computer code, along with $\alpha$ and m for the determination of wake growth in the various regions.

Region IV wake growth is determined only by the value of the dispersion due to the ambient turbulence, $\alpha$.

## 2.3 Geometry of Wake Regions

Figure 2-3 presents the characteristic wake lengths and radii for the four regions. Wake growth is assumed to be linear in each of the regions. The relationships between the various geometrical and flow parameters are given below:

### Velocities

free stream velocity:

$$U_o$$

initial wake velocity (fully expanded slipstream):

$$U_{mo} = V_{\infty, \text{BERNOULLI}}$$

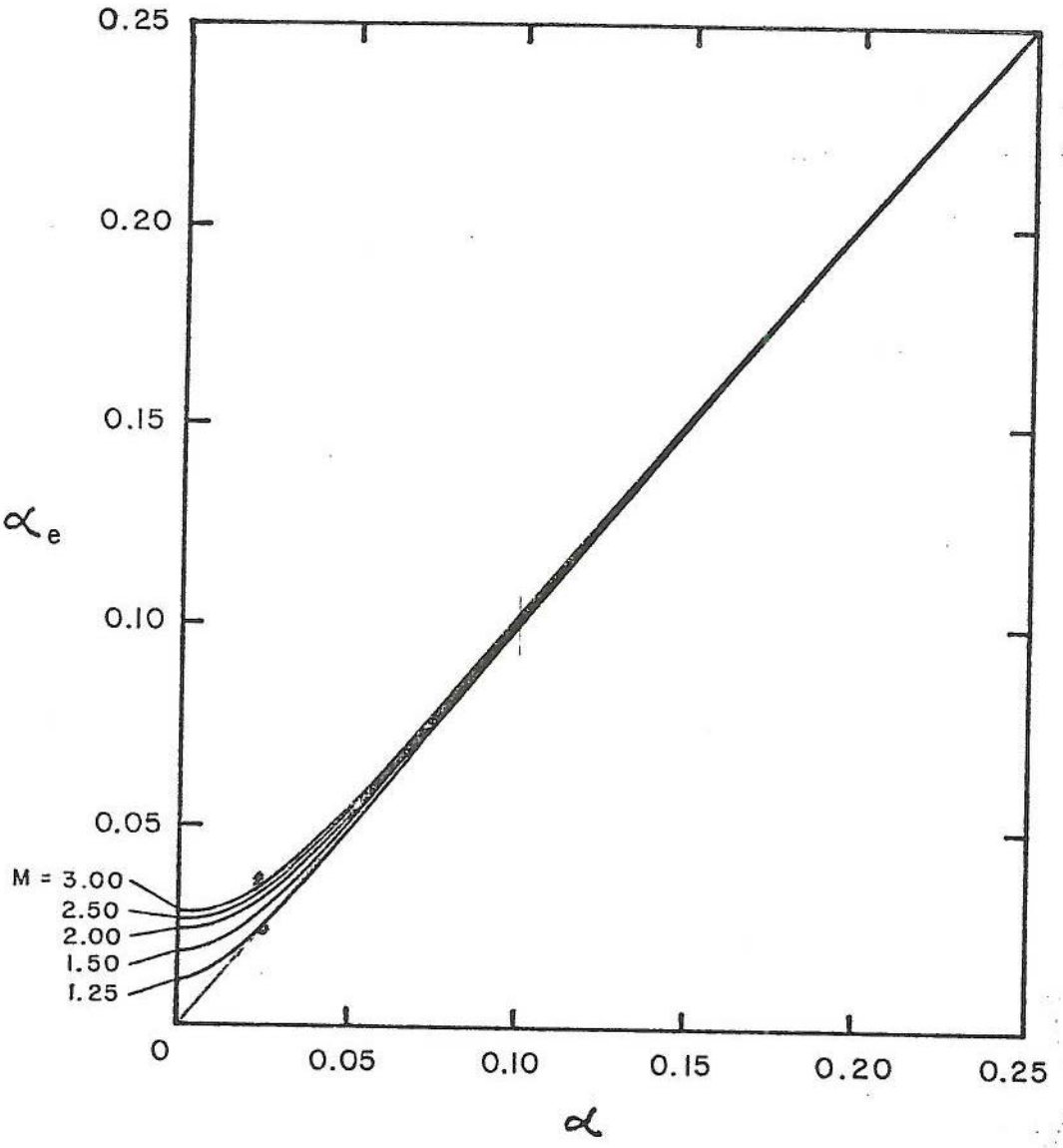


FIGURE 2-2. Effective wake dispersion parameter in Region III.

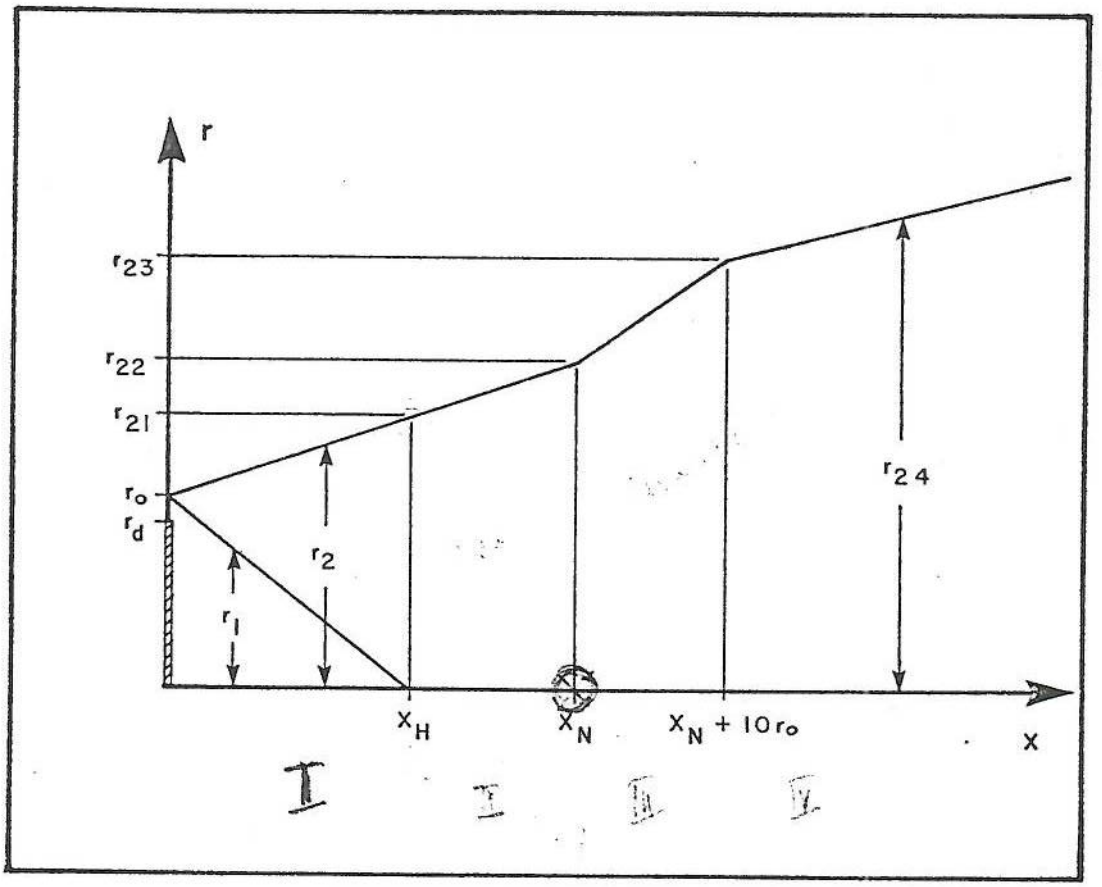


FIGURE 2-3. Characteristic wake parameters.

flow velocity ratio:

$$m = \frac{U_o}{U_{mo}}$$

initial wake velocity decrement:

$$\Delta U_{mo} = U_o \left(1 - \frac{1}{m}\right)$$

Downstream Distances

$$\frac{X_H}{r_o} = \frac{1}{\sqrt{\left(\frac{\alpha}{.51}\right)^2 + \left[\frac{(1-m)\sqrt{1.49+m}}{9.76\,(1+m)}\right]^2}}$$

which is taken from Eqn. (5.20) in Abramovitch with the ambient growth term $\alpha/.51$ added.

The basis of this algorithm is that the rate of inner core erosion by mechanical turbulence is taken from Abramovitch, and this rate is augmented by combining the rate of ambient turbulence erosion according to the combination rule of taking the square root of the sum of the squares. The outer wake radius is connected to the core radius by the momentum deficit relations. This particular model can result in a non-monotonic wake growth rate, that is the wake growth rate before the main jet has developed may be some what lower than the intermediate growth rate. This is somewhat unexpected behavior, since one would expect the growth rate to continually reduce with downstream distance. However, it is noted that this behavior is theoretically predicted, (see Figure 5.17 of Abramovitch) and in addition, there is good experimental evidence of this as demonstrated by Figure 5.37 of Abramovitch. This point is discussed further in section 3.1.

For the second region:

$$X_N = nX_{H'}$$

where:

$$n = \frac{\sqrt{.214 + .144\,m}}{1 - \sqrt{.214 + .144\,m}} \quad \frac{1 - \sqrt{.134 + .124\,m}}{\sqrt{.134 + .124\,m}}$$

as given in Eqn. (5.124) from Abramovitch.

Wake Radii

Wake growth rate for each region is implicitly contained in the following expressions. The ratio of slipstream diameter, $r_o$, to the disk diameter, $r_d$ is given by the well-known actuator disk result:

$$\frac{r_o}{r_d} = \sqrt{\frac{m+1}{2}}$$

The outer radius at the end of Region I is given by Abramovitch's Eqn. (5.21') which can be written in the form: from Abramovitch

$$\frac{r_{21}}{r_o} = \frac{-a + \sqrt{a^2 + 4b}}{2b} = \frac{1}{\sqrt{0.214 + 0.144m}}$$

where: $a = .416 + .134\,m$

$b = (.021)(1 + .8m - .45\,m^2)$

The radius at the end of the transition region, $r_{22}$, assuming the same growth rate as in Region I is then given by:

$$\frac{r_{22}}{r_o} = 1 + n\left(\frac{r_{21}}{r_o} - 1\right)$$

In Region III, which has the local growth rate $\alpha_e/.51$, we get:

$$\frac{r_{23}}{r_o} = \frac{r_{22}}{r_o} + 10\,K\,\frac{\alpha}{.51}$$

where: $K = \frac{\alpha_e}{\alpha}$.

Finally, in Region IV, at a growth rate of $\alpha/.51$, we get:

$$\frac{r_{24}}{r_o} = \frac{r_{23}}{r_o} + \frac{\alpha}{.51}\,(X - X_N - 10\,r_o)$$

## 2.4 Velocity Profiles

The velocity profiles in the various wake regions are taken directly from Abramovitch (1963) and are, for the near wake, $\Delta U/\Delta U_m = (1 - \eta^{1.5})^2$, where $\eta = (r_2 - r)/(r_2 - r_1)$, for $r > r_1$, and $\Delta U = \Delta U_{mo}$, for $r \leq r_1$, and for the far wake, $\Delta U/\Delta U_m = (1 - \xi^{1.5})^2$, where $\xi = r/r_{24}$. Outside of the outer wake radius, $\Delta U = 0$. In the transition region, the velocity profile was taken as a linear combination of the near wake and far wake profiles that exist at the beginning and the end of this region. Although this does not exactly satisfy the conservation of drag in this region, a series of integrations of these synthesized velocity profiles were performed to determine the extent of the departure of the drag in the transition region. These

integrations were performed over a range in downstream distance in the transition region and over a range in the wind turbine power coefficent, represented by the velocity ratio, m. In most cases, the calculated drag using this simple model was within 1% of the actual value and the largest departure was 3%. Thus, this method of determining transition region velocity profiles was deemed satisfactory. Figure 2-4 shows the velocity profiles from all the regions drawn to the same scales for both radius and centerline velocity decrement, respectively. The profile shown for the transition region was selected from the position midway between the end points of the region.

In the initial region (Region I), $\Delta U_m / \Delta U_{mo} = 1$, and in the far wake regime, the centerline velocity decrement is related to the outer wake radius,

$$\Delta \bar{U} = \frac{\Delta U_m}{\Delta U_{mo}} = \frac{-.258\ m + \sqrt{(.258\ m)^2 + .536(1 - m)\left(\frac{r_o}{r_{24}}\right)^2}}{.268\ (1 - m)},$$

which is obtained by manipulation of Eqn. 5.97 in Abramovitch.

## 2.5 Addition of Velocities

In areas of wake overlap, the resulting total velocities were obtained by adding the calculated velocity decrements for each wind turbine and subtracting from free stream speed. This implies that the velocity defect can be regarded as a scaler convected by turbulent fluctuations which are not themselves functions of this velocity.

For the situation in which a wake generating turbine (turbine 1) was itself in the wake of a farther upstream mechine (turbine 2), the following rule was used. The input velocity profile to turbine 1 due to the wake of turbine 2 was calculated. From this, the average input velocity was determined by numerical integration of the wake velocities of turbine 2 across the disk of turbine 1, as described in Section 2.7.

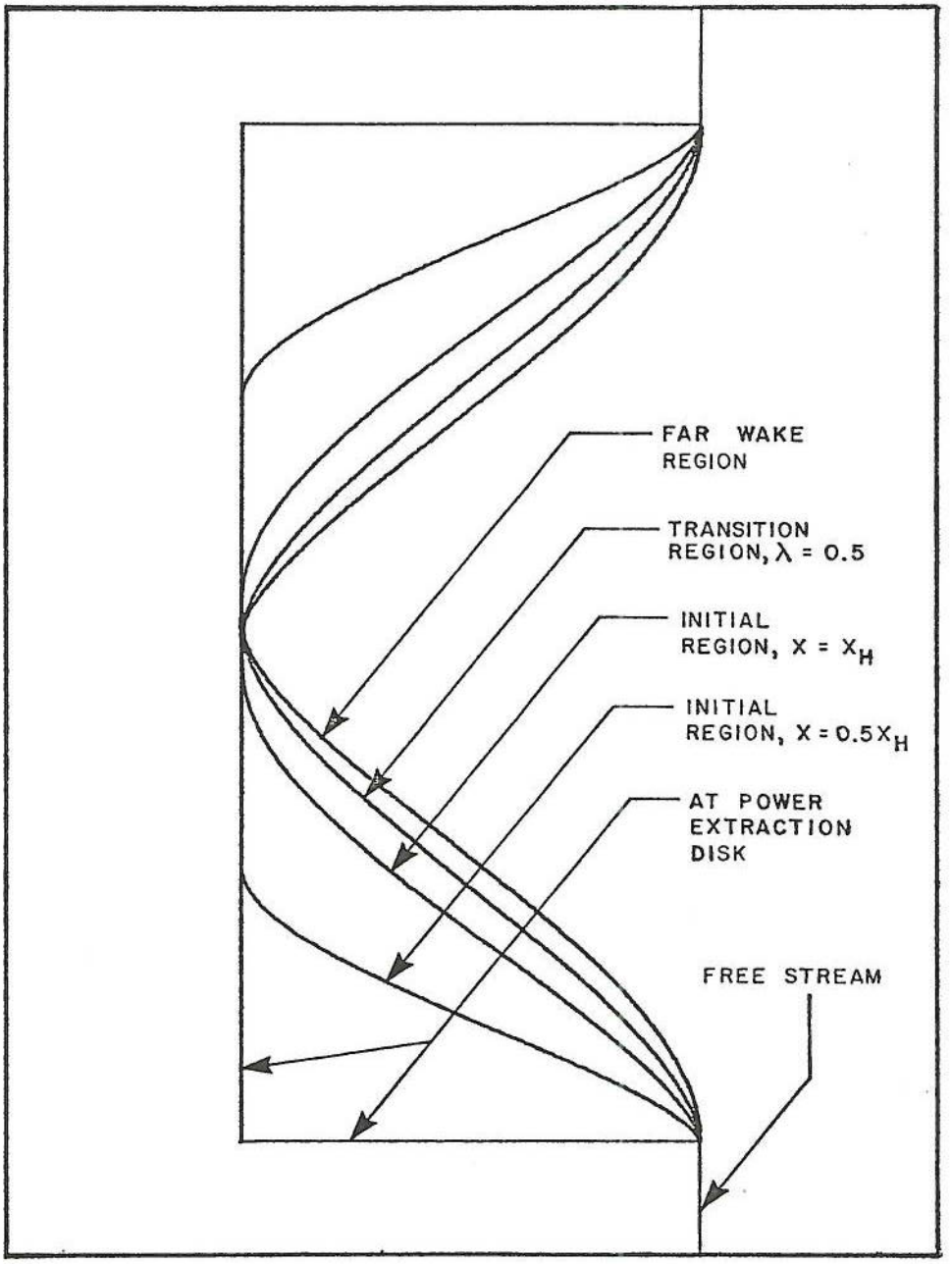


FIGURE 2-4. Velocity profiles in the various wake regions.

The ratio formed between this average input velocity and the free stream velocity was then used to scale all resulting velocity decrements when subsequent wake analysis was performed on turbine 1. These properly scaled velocity decrements were then used to perform subsequent operations at downstream locations influenced by turbine 1.

## 2.6 Ground Plane

The effect of the ground plane was modeled by placing an image turbine at a distance below the ground plane equal to the height above the ground of the actual mechine. This produced two parallel, offset, and eventually overlapping wakes, oriented vertically as shown in Figure 2-5. The velocity decrements from the two wakes were added in the manner described previously in Section 2.5 for the overlapping of conventional wakes.

## 2.7 Integration of Power and Average Velocity across Receptor Disk

To determine the velocity and power flux across the disk of an arbitrary receptor wind turbine first requires that the velocity decrements due to all upstream sources and their images be determined and properly summed to determine the absolute velocity at every point on the surface of the receptor disk called for by the integration routine. The addition of wake velocity decrements due to overlapping wakes and image wakes has already been discussed. Figure 2-6 shows the grid used at the receptor disk to perform the numerical integration.

Two quantities were determined by this integration process. First, the absolute velocity was found at the center of each square on the grid. These velocities were all divided by free stream velocity. Summing and dividing by the total number of integration points, gave the average inlet velocity (referenced to free stream velocity) for the receptor disk. Cubing the velocities and dividing each by the cube of the free stream velocity before summing resulted in the input power ratio, again referenced to free stream available power.

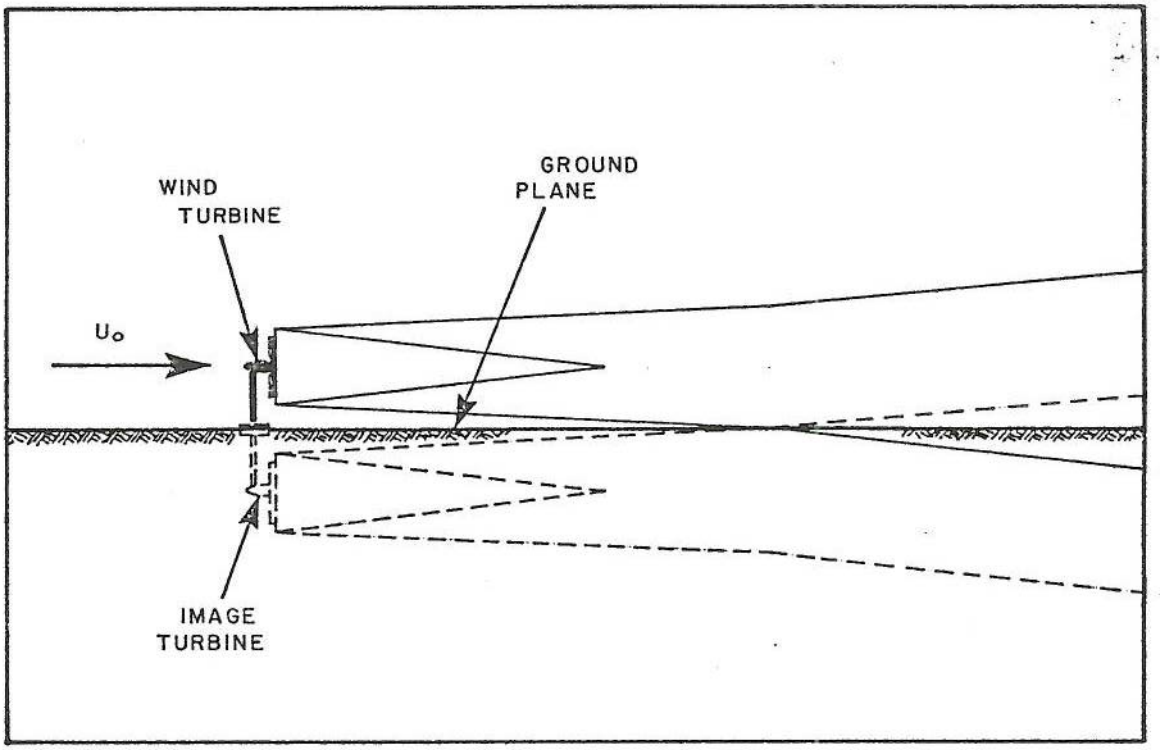


FIGURE 2-5. Image representation of ground plane.

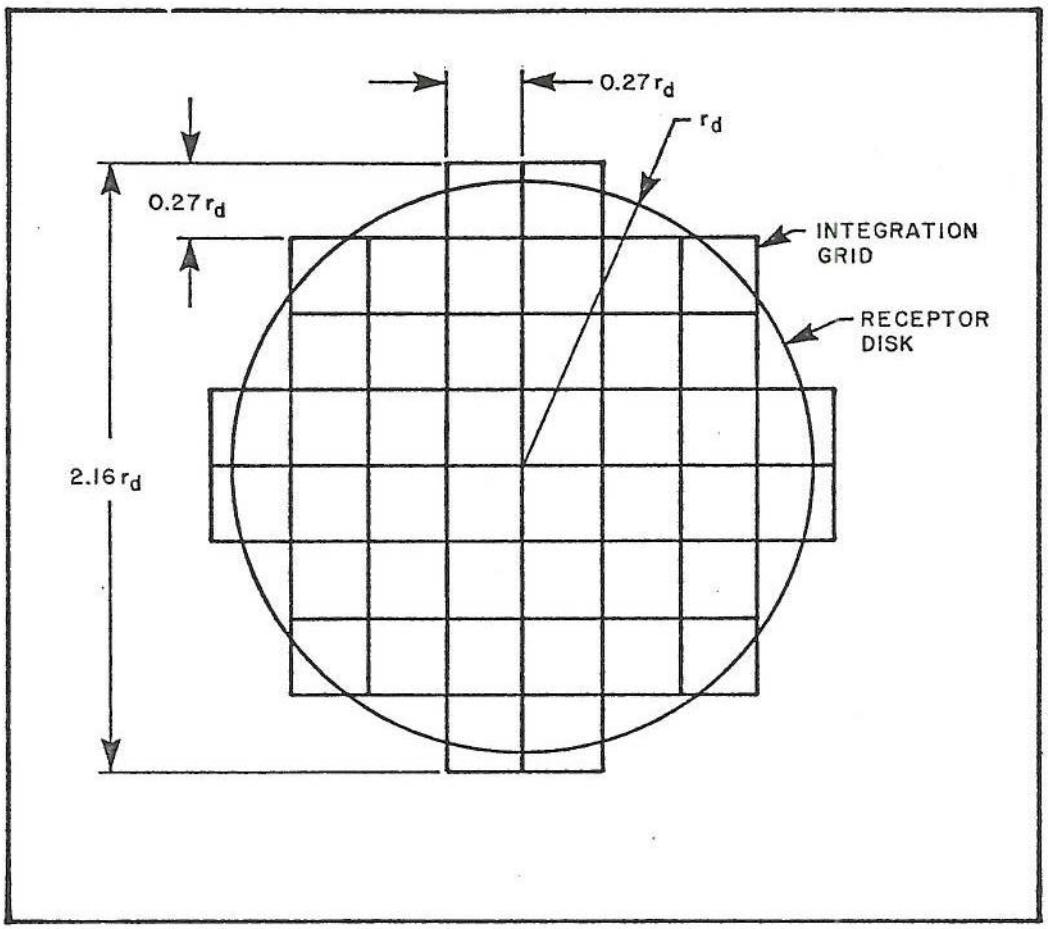


FIGURE 2-6. Receptor disk integration grid.

## 2.8 Array Geometry

The program developed here is capable of handling an array of wind turbines of arbitrary geometry with arbitrary wind direction. Two different cartesian coordinate systems are used in the program. The first is the geographical coordinates in which the positions of each of the wind turbines are specified for a system fixed with respect to the points of the compass. Thus, in this rectangular coordinate system, the y-axis is oriented north and the orientation of the wind vector is measured clockwise from this direction.

In order to compute the overall wake geometry for the wind turbines in the array, a transformation (rotation) or coordinates is performed to a windwise system in which the wind enters the array along the negative x-direction. All of the positions of each of the wind turbines in the array are re-calculated for this new coordinate system, while at the same time preserving the unique interrelationship of the geometry of the array. It is assumed that the wind turbines are capable of weathercock motions, so that their power extraction disks are always perpendicular to the direction of the entering wind.

For "bookkeeping" purposes in the program, the individual wind turbines in the transformed array are numbered in the direction of increasing downwind distance. This defines the order in which all of the wind turbines (or wind turbine rows) are encountered by the moving air stream.

Figure 2-7 shows the two coordinate system used for the relatively simple example of a square array of wind turbines. In all cases, the distances are non-dimensionalized by the radius of the windmill disk, $r_d$. The cross stream coordinate, y, is not uniquely specified for the transformed coordinate system since it is positioned with respect to each of the wind turbines in turn as each is considered as the receptor by the program. Thus, the "origin" of the transformed coordinate system is placed in turn at each of the wind turbines. Only those wind turbines upstream (with a lower

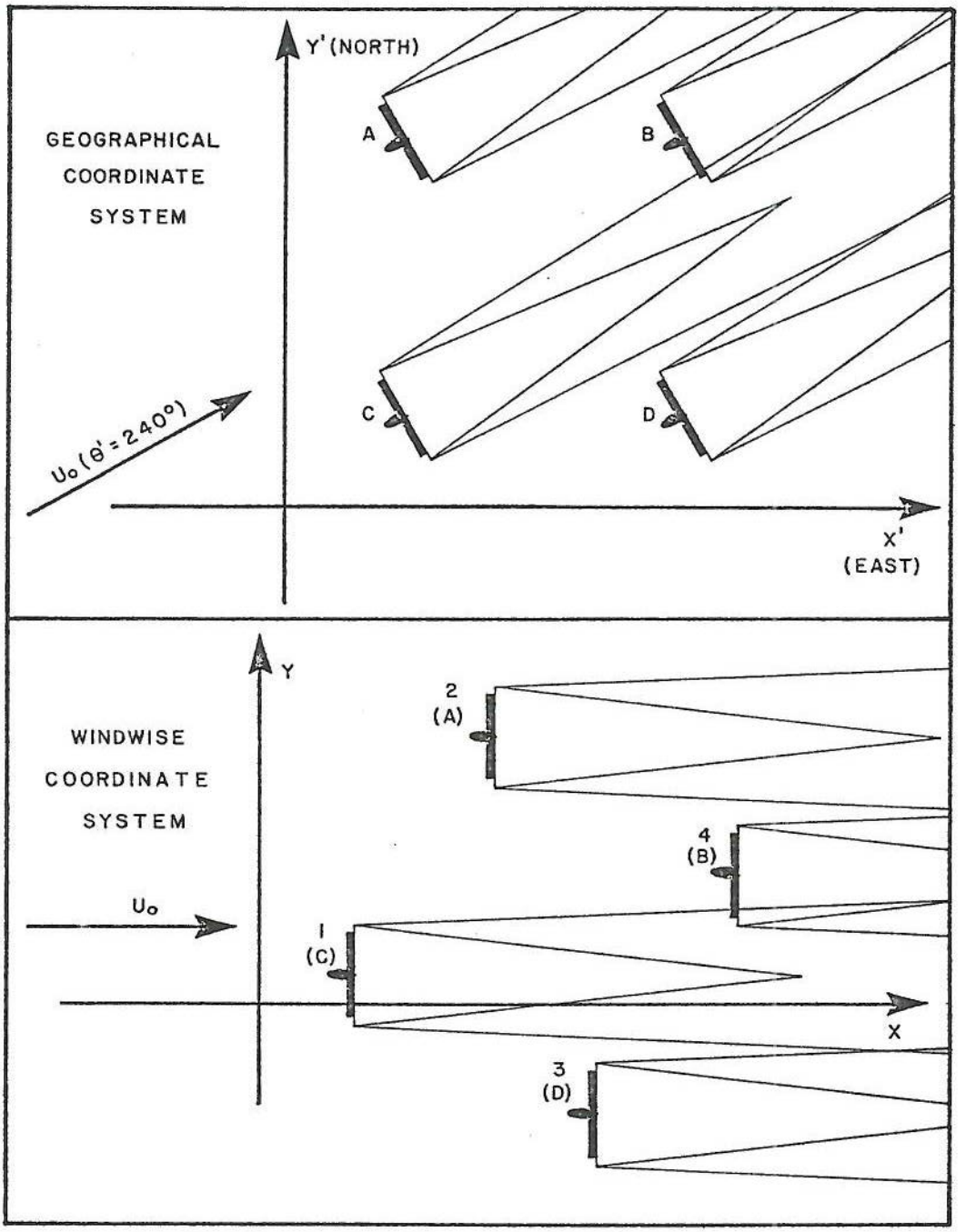


FIGURE 2-7. Coordinate systems used in the computer program.

number in the numbering scheme) are considered by the program to influence the receptor.

## 2.9 Summation of Array Elements

As previously mentioned, each of the wind turbines is considered as a receptor and its average entering velocity and power ratio is calculated by the program. The average power ratio for the entire array is easily obtained by summing the power ratios for each of the wind turbines and dividing by the total number.

Section 2.5 and 2.6 describe the method by which the total entering velocity profile is determined for any given wind turbine due to the effects of the upstream generated wakes and images produced by the other pertinent wind turbines in the array.

The program determines which are "pertinent" by the following method. First, of course, a pertinent wind turbine must be upstream of the wind turbine being considered as receptor. As previously discussed, this is easily determined by the windwise numbering system employed by the program during the transformation of coordinates. Secondly, the wake of a pertinent upstream wind turbine must have expanded sufficiently in the cross-wind direction (for the particular downstream station at which the receptor is located) that it completely or partially intercepts the disk of the receptor. Upstream wind turbines for which this is not the case need not be considered. Here, a conservative approximation was employed for this determination, described in the following paragraphs.

The maximum wake growth rate occurs in Region III. Figure 2-8 shows this growth rate originating from the receptor disk and extending upstream as a "zone of influence." By definition, any wind turbines or parts of wind turbines contained within this zone of influence from the receptor may themselves have real wakes that extend downstream and intercept the receptor. Thus, this upstream zone of influence establishes the geometrical

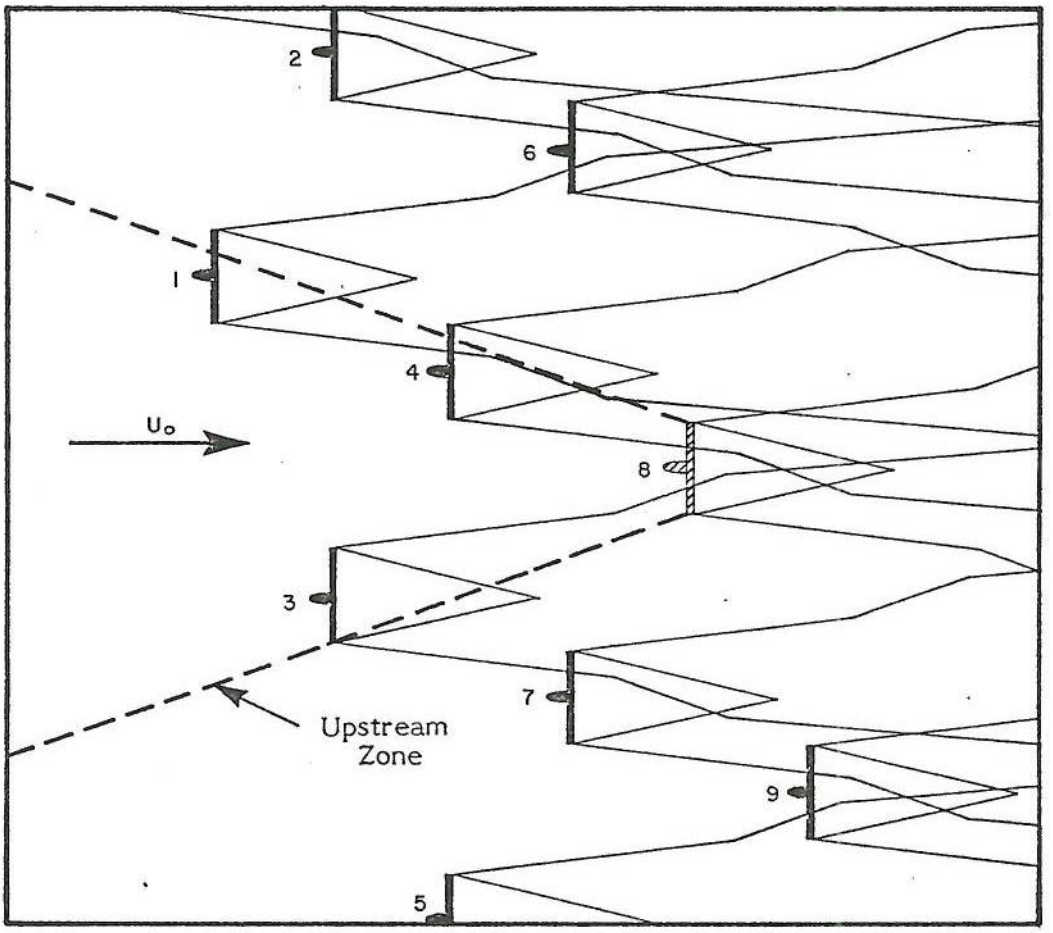


FIGURE 2-8. Upstream zone of influence.

criterion that was used by the program to eliminate upstream wind turbines that will have no effect on the particular receptor being considered. This method was used for each wind turbine in the array in turn, when considered as receptor.

As stated previously, this method of elimination is conservative, since over most of the downstream distance of the wake the growth rate is less than in Region III. Thus, some wind turbines may be included in the subsequent wake velocity determination routine which actually have no influence – but none will be missed. The objective of this entire exercise is only to speed up the calculation routine, since in an array of many wind turbines, most often only the wakes from relatively few of them actually influence a particular receptor for many of the wind angles encountered. In any event, the program always includes in a proper fashion all of the wind turbines that influence the performance of a given, downwind receptor.

## 2.10 Program Logic

The computer logic was developed on the Hewlett Packard HP 9820A minicomputer because of ease of manipulation of the machine during the writing and "debugging" stage. After the program was proven to perform satisfactorily on this machine, it was transcribed into FORTRAN IV format for universal use on larger and faster machines.

Figures 2-9 through 2-11 are flowcharts of the final, FORTRAN program. The complete listing of the FORTRAN program including all subroutines is included in Figure 2-12.

The program consists of a main program with eight subroutines. Because of the similarity between the FORTRAN and the Hewlett Packard 9820A programs, only the FORTRAN version is presented here. In any case, the H.P. version should only be considered as a developmental tool, while the FORTRAN is the fully functional version. It can presently handle an array of up to 100 wind turbines, but can be expanded easily to any size array, the only limitations being computer memory and computation time.

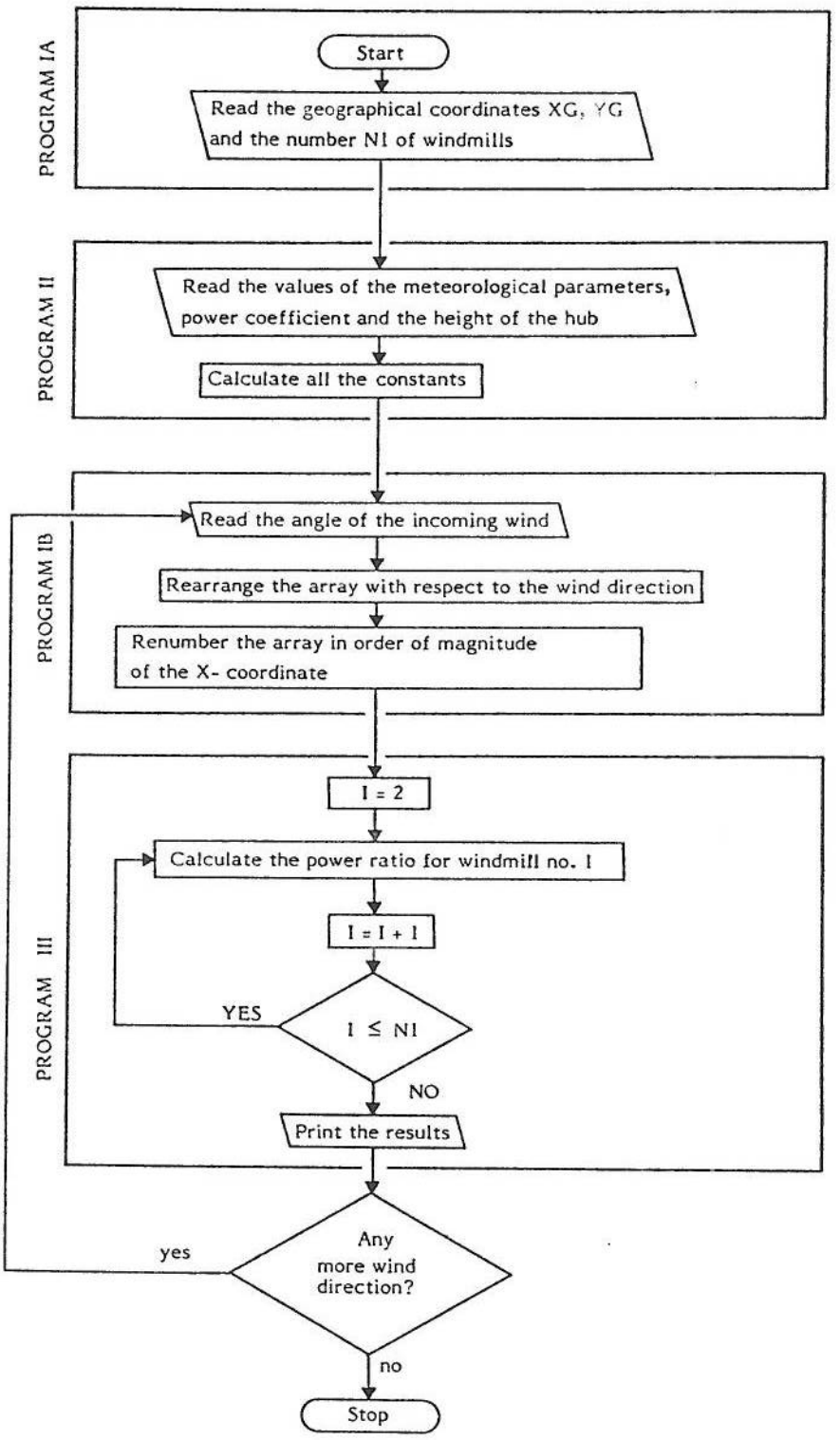


FIGURE 2-9. Computer flowchart for coordinate transformation routine.

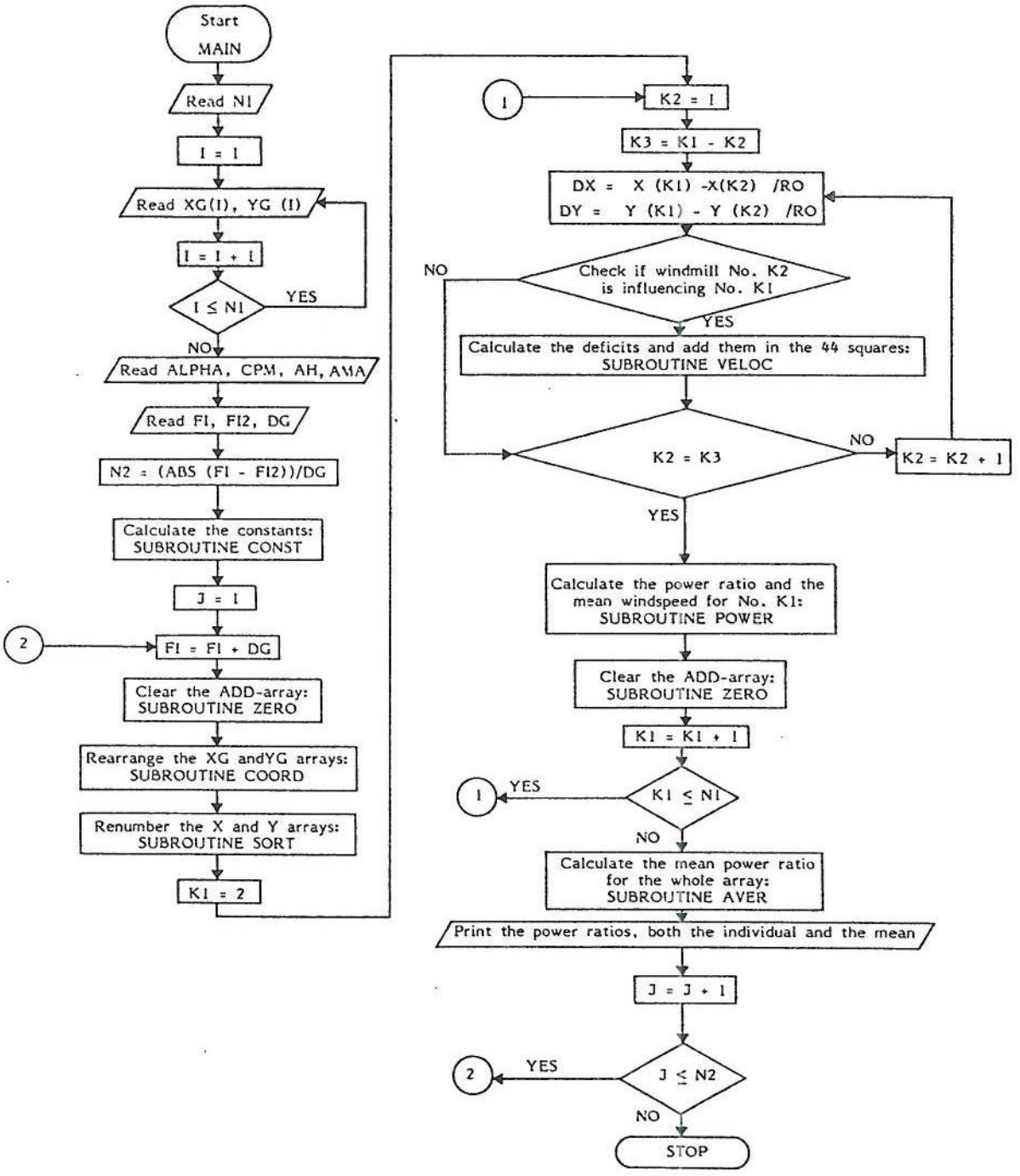


FIGURE 2-10. Computer flowchart for array power ratio.

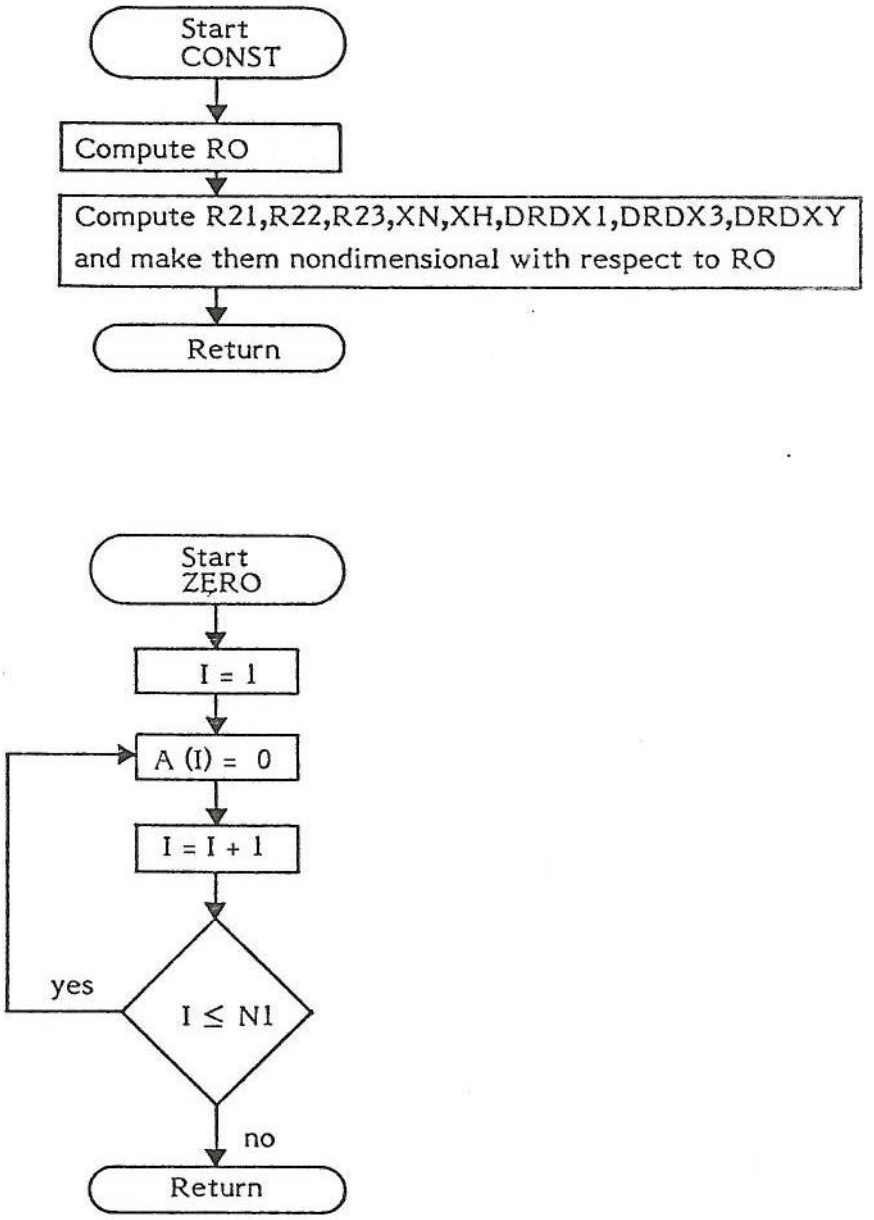


FIGURE 2-11. Subroutines involved in array power ratio program.

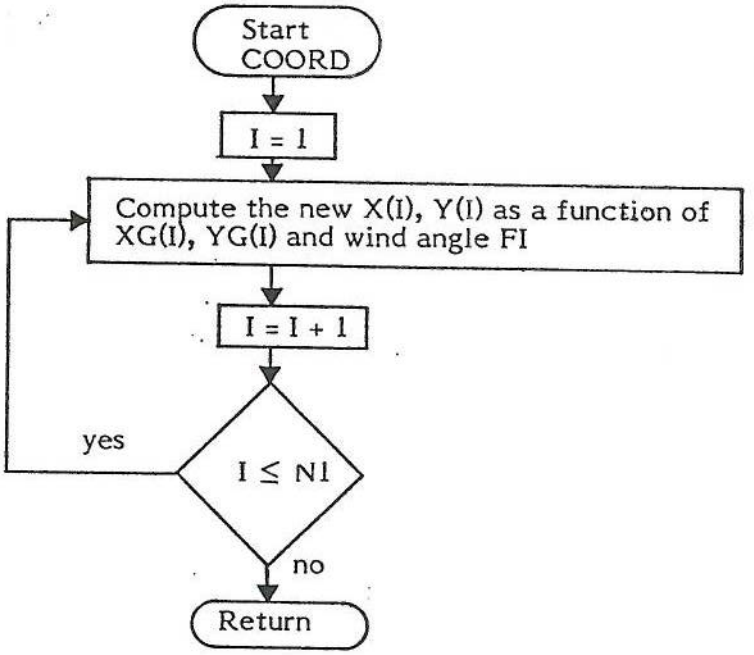


FIGURE 2-11. (Continued)

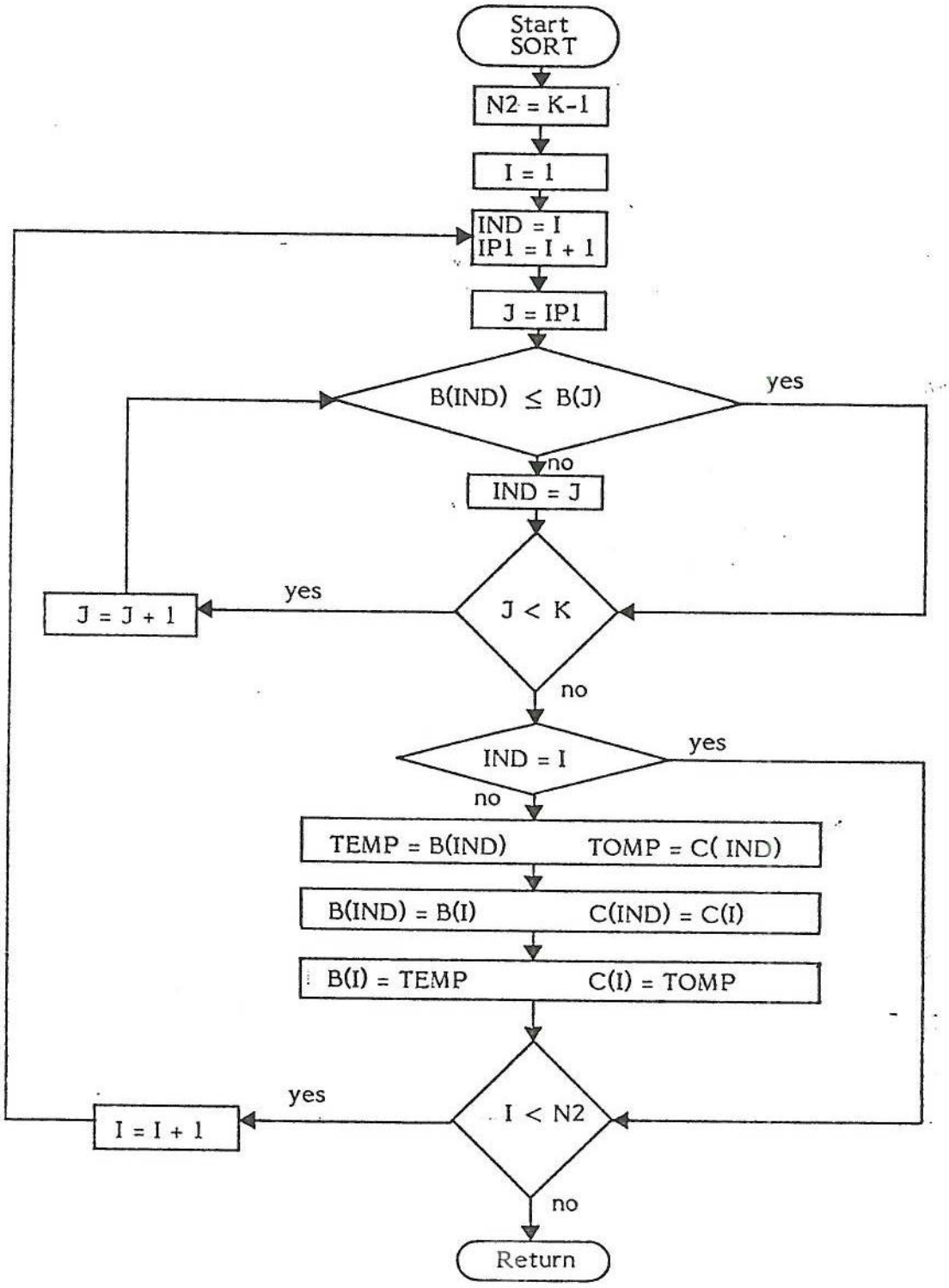


FIGURE 2-11. (Continued)

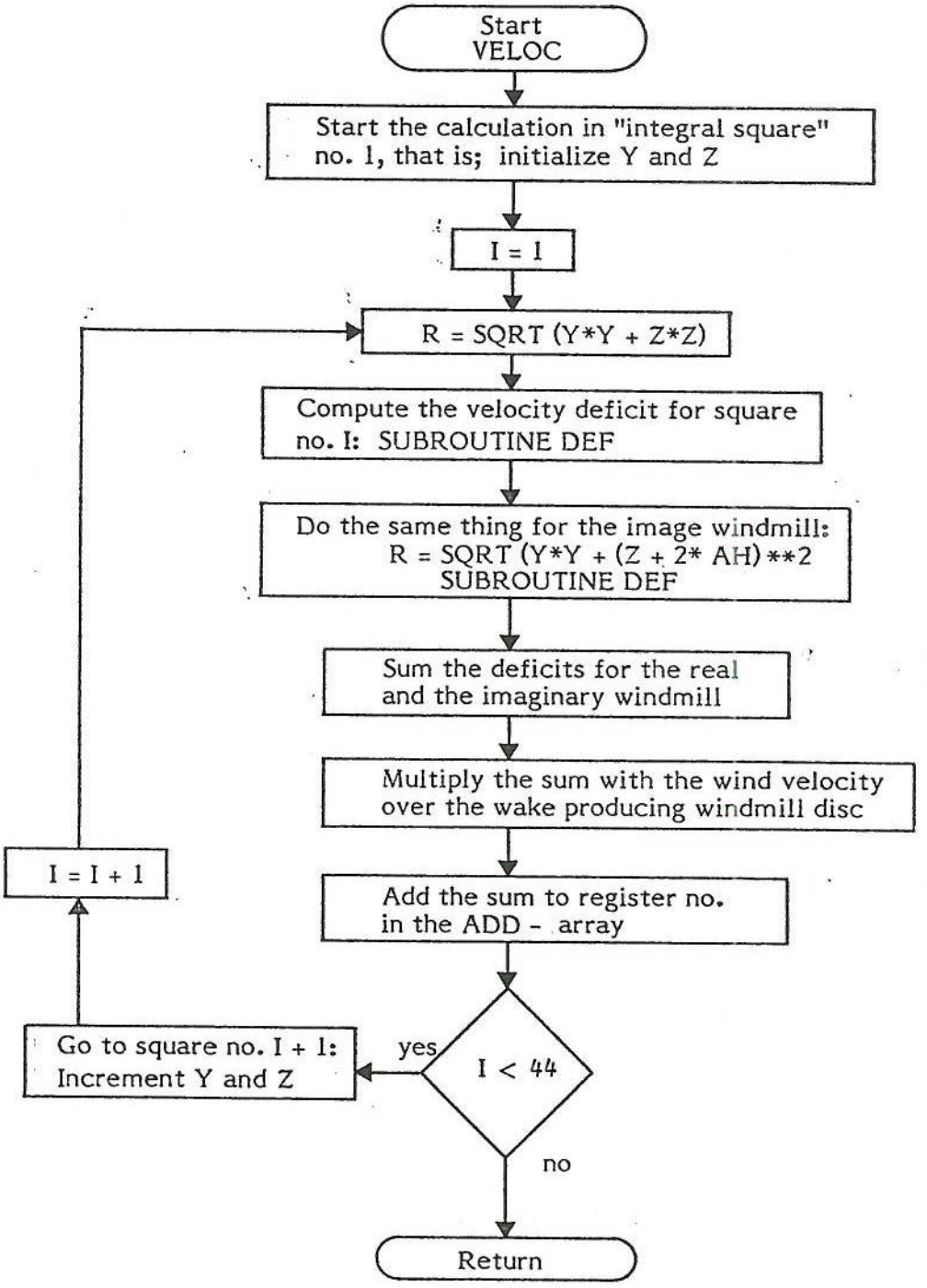


FIGURE 2-11. (Continued)

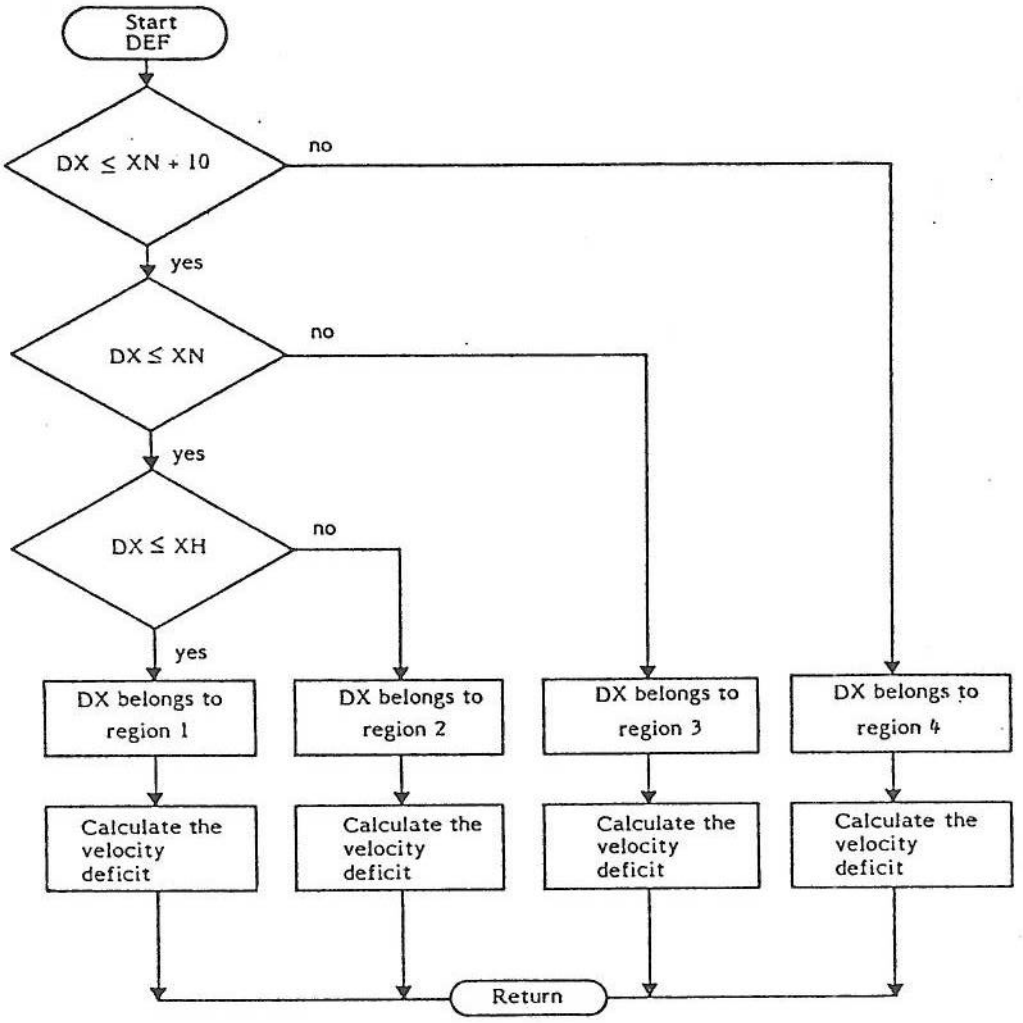


FIGURE 2-11. (Continued)

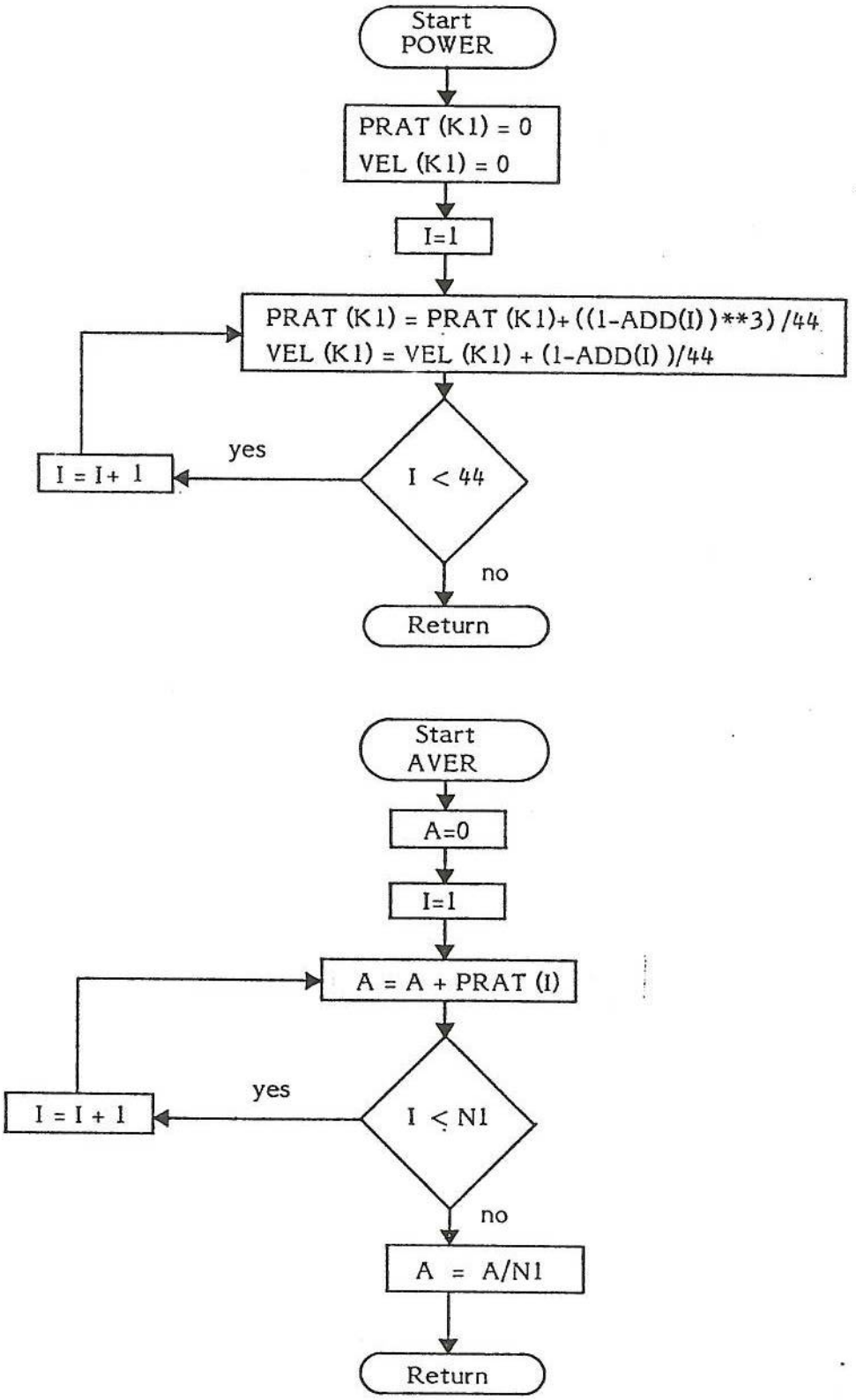


FIGURE 2-11. (Concluded)

```
C     ****************************************************************
C     *                                                              *
C     *                                                              *
C     *     PROGRAM: WIND                              08/APR/77     *
C     *                                                              *
C     *     WECS ARRAYS ANALYSIS PERFORMED FOR THE SWEDISH           *
C     *     BOARD OF ENERGY.                                         *
C     *     THIS VERSION WRITTEN FOR THE HEWLETT-PACKARD             *
C     *     21-MX OPERATING UNDER DOS-M.                             *
C     *                                                              *
C     *     AEROVIRONMENT INC.          TORGNY FAXEN, PROGRAMER      *
C     *                                                              *
C     *                                                              *
C     ****************************************************************
C
C
      PROGRAM WIND
      DIMENSION ADD(44),NR(100),CO(6),VEL(100),PRAT(100)
      DIMENSION TITL(20)
      COMMON XG(100),YG(100),X(100),Y(100)
C
C     READ TITLE CARD
C
      READ(5,500)TITL
500   FORMAT(20A4)
      WRITE(6,501)TITL
501   FORMAT(1H1,20A4/)
C
C     READ THE AMOUNT OF WINDMILLS
C
      READ(5,100)N1
100   FORMAT(I2)
      WRITE(6,902)N1
902   FORMAT(" THE "I2" WINDMILL COORDINATES"//6X"X"9X"Y"/)
C
C     READ THE (X,Y) COORDINATES FOR ALL THE WINDMILLS
C
      DO 120 I=1,N1
      READ(5,110)XG(I),YG(I)
      WRITE(6,110)XG(I),YG(I)
110   FORMAT(2F10.4)
      NR(I)=I
120   CONTINUE
C
C      READ ALPHA,M,HEIGHT,ALPHA EFFECTIVE
C
      READ(5,130)ALPHA,CPM,AH,AMA
      WRITE(6,132)ALPHA,CPM,AH,AMA
132   FORMAT("0INPUT VARIABLES"//" ALPHA= "F10.4" CPM= "F10.4
     *       " AH= "F10.4" AMA= "F10.4)
130   FORMAT(4F10.4)
```

FIGURE 2-12. Listing for FORTRAN program for wind turbine array power ratio.

```
C       WE NOW HAVE ALL THE NECESSARY DATA
C       EXCEPT THE WIND DIRECTION, READ
C       WIND DIRECTION FOR START AND STOP AND
C       LENGHT OF EACH STEP

        READ(5,160)FI,FI2,DG
160     FORMAT(3F10.4)
        WRITE(6,162)FI,FI2,DG
162     FORMAT(" FI= "F10.4" FI2= "F10.4" DG= "F10.4//)
C
C       CALCULATE HOW MANY STEPS THERE ARE
C
        N2=(ABS(FI-FI2))/DG+0.5+1
C
C       CALCULATE ALL THE CONSTANTS
C
        CALL CONST(ALPHA,CPN,AH,AMA,R0,R01
       1,R21,R22,R23,XN,XH,DRDX1,DRDX3,DRDX4,C0)
        WRITE(6,170)XN,R0,R21,R22,R23,DRDX1,DRDX3,DRDX4
 170     FORMAT(4X"XN= "F5.2" R0= "F5.2" R21= "F5.2" R22= "F5.2
      *   " R23= "F5.2" DRDX1= "F5.2" DRDX3= "F5.2" DRDX4= "F5.2/)
C
C       START THE CALCULATION OF POWER RATIO
C       FOR EACH WIND MILL
        FI=FI-DG
C
        PRAT(1)=1.
        DO 250 IFI=1,N2
        FI=(FI+DG)*2.*3.1415962/(360.)
C
C       EMPTY THE ARRAY FOR THE VELOCITY PROFILES
C
        CALL ZERO(ADD,44)
C
C       REARRANGE THE ARRAY WITH RESPECT TO
C       INCOMING WIND
C
        CALL COORD(FI,N1)
C
C       RENUMBER THE ARRAY
C
        CALL SORT(N1,NR,X,Y)
C
C       CONTINUE THE CALCULATIONS OF THE POWER RATIO
C
        DO 215 K1=2,N1
        K2=1
        K3=K1-K2
```

FIGURE 2-12. (Continued)

```
      DO 210 K2=1,K3
      DX=(X(K1)-X(K2))/RO
      DY=(-Y(K2)+Y(K1))/RO
      IF(DX.GE.0)GO TO 200
      WRITE(9,205)
205   FORMAT(1X,"ERROR")
      STOP
C     CHECK IF WINDMILL NUMBER K2
C     IS INFLUENCING NUMBER K1, IF
C     NOT PRINT THAT OUT AND JUMP TO THE
C     NEXT WINDMILL
C
200   IF((ABS(DY)-2.*1.)/(ABS(DX)+0.00001).GT.DRDX3)GO TO 210
C
C     CALCULATE THE DEFICIT FOR ALL THE 44
C     SQUARES AND ADD TO THE PREVIOUS CALCULATED.
C
      CALL VELOC(K2,CPM,AH,RD1,R21,R22,R23,XM,XH,DRDX1
     2,DRDX3,DRDX4,CO,DX,DY,VEL,ADD)
210   CONTINUE
C
C     WE HAVE NOW CALCULATED THE DEFICITS FROM
C     ALL THE WINDMILLS THAT INFLUENCED K1
C     NOW WE MUST CALCULATE THE POWER RATIO
C     AND THE AVERAGED VELOCITY OVER THE DISC.
C
      CALL POWER(K1,VEL,PRAT,ADD)
C
C     EMPTY THE REGISTERS BEFORE NEXT ROUND
C
      CALL ZERO(ADD,44)
215   CONTINUE
      CALL AVER(N1,P,PRAT)
C
C     WE HAVE NOW CALCULATED THE
C     POWER RATIOS FOR ALL THE WINDMILLS IN
C     THE ARRAY FOR A GIVEN WIND-DIRECTION
C     WE SHALL NOW PRINT THE RESULTS.
C
      WRITE(9,230)
230   FORMAT("0,**************************************************'
     *"**********************************************")
      FI=FI*360./(2*3.1415926)
      WRITE(9,240)FI
240   FORMAT(8X,"X",11X,"Y",7X,"P-RAT",10X,"WIND-DIRECTION",
     3 F6.0)
      DO 260 I=1,N1
      K=NR(I)
      WRITE(9,280)XG(K),YG(K),PRAT(I)
280   FORMAT(5X,3F10.4)
      NR(I)=I
260   CONTINUE
      WRITE(9,290)P
290   FORMAT(44X,"AVERAGED POWER RATIO FOR "
     4 "THE WHOLE ARRAY =",F5.3  )
C
```

FIGURE 2-12. (Continued)

```
C       RETURN TO THE BEGINNING TO SEE IF THERE
C       ARE ANY MORE WIND DIRECTIONS TO CALCULATE THE
C       POWER RATIOS FOR
C
250     CONTINUE
        END
```

```
C
C       CALCULATION OF CONSTANTS
C
        SUBROUTINE CONST(ALPHA,CPM,AH,AMA,RO,RD1,R21,R22
       1,R23,XN,XH,DRDX1,DRDX3,DRDX4,CO)
        DIMENSION CO(6)
        RD1=1.
        RO=RD1*SQRT((CPM+1.0)/2.0)
        CO(1)=0.416+0.134*CPM
         CO(2)=0.021*(1.0+0.8*CPM-0.45*(CPM*CPM))
        CO(3)=SQRT(0.214+0.144*CPM)
        XH=1.0/SQRT((ALPHA/0.51)**2+(0.27*(1.0-CPM)*CO(3)/(1.0+CP
      *   **2)
        CO(4)=SQRT(0.134+0.124*CPM)
        R21=(-CO(1)+SQRT(CO(1)*CO(1)+4.0*CO(2)))/(2.0*CO(2))
        DRDX1=(R21-1.)/XH
        CO(6)=CO(3)*(1.0-CO(4))/((1.0-CO(3))*CO(4))
        R22=1.+CO(6)*(R21-1.)
        XN=CO(6)*XH
        DRDX3=ALPHA*AMA/0.51
        R23=R22+10.0*DRDX3
        DRDX4=ALPHA/0.51
        RD1=RD1/RO
        AH=AH/RO
        RETURN
        END
```

```
C       RESET STORAGE ARRAY TO ZERO
C
        SUBROUTINE ZERO(A,N)
        DIMENSION A(44)
        DO 20 I=1,N
        A(I)=0.
20      CONTINUE
        RETURN
        END
```

FIGURE 2-12. (Continued)

```
C
C       REARRANGE THE ARRAY WITH RESPECT TO THE INCOMING WIND
C
        SUBROUTINE COORD(FI,N1)
        COMMON XG(100),YG(100),X(100),Y(100)
        DO 20 I=1,N1
        R=SQRT(XG(I)*XG(I)+YG(I)*YG(I))
        IF(0.00001.GE.XG(I).AND.XG(I).GE.-0.0001)XG(I)=0.00005
        A=ATAN(YG(I)/XG(I))
        IF(XG(I).LT.0.)A=A+3.1415926
        Y(I)=R*COS(A+FI)
        X(I)=-R*SIN(A+FI)
20      CONTINUE
        RETURN
        END


C
C       RENUMBER THE ARRAY
C
        SUBROUTINE SORT(K,M,B,C)
        DIMENSION M(100),B(100),C(100)
        N2=K-1
        DO 40 I=1,N2
        IND=I
        IP1=I+1
        DO 50 J=IP1,K
        IF(B(IND).LE.B(J))GO TO 50
        IND=J
50      CONTINUE
        IF(IND.EQ.I)GO TO 40
C
C       CHANGE PLACES
C
        TEMP=B(IND)
        TOMP=C(IND)
        L=M(I)
        M(I)=M(IND)
        M(IND)=L
        B(IND)=B(I)
        C(IND)=C(I)
        B(I)=TEMP
        C(I)=TOMP
40      CONTINUE
        RETURN
        END
```

FIGURE 2-12. (Continued)

```
C
C       CALCULATE THE DEFICIT
C
        SUBROUTINE DEF(R,VINT,RD1,R21,R22,R23,XN,XH,DRDX1,DRDX3
       1,DRDX4,CO,DX,CPM)
        DIMENSION CO(6)
        IF(XN+10..LE.DX)GO TO 10
        IF(XN.LE.DX)GO TO 20
        IF(XH.LE.DX)GO TO 30
C
C       DX BELONGS TO REGION 1
C
        R1=1.-DX/XH
        R2=1.+DX*DRDX1
        IF(ABS(R1-R2).LE.0.00001)R2=R1+0.000001
        ETA=(R2-R)/(R2-R1)
        IF(ETA.GE.0.)GO TO 35
C
C       ETA LESS THAN 0, THAT MEANS R GREATER THAN R2
C       WHICH MEANS THAT WE ARE OUTSIDE THE WAKE AND
C       DU EQUALS ZERO
C
        VINT=1.
        GO TO 100
35      IF(ETA.LE.1)GO TO 40
C
C       ETA GT 1 WHICH MEANS THAT R LT R1 WHICH
C       MEANS THAT WE ARE IN THE CORE REGION
C
        VINT=1./CPM
        GO TO 100
40      VINT=(1.-(1.-CPM)*(1.-ETA**1.5)**2)/CPM
        GO TO 100
C
C       DX BELONGS TO TRANSITION REGION
C
30      R2=1.0+DX*DRDX1
        DU=-0.258*CPM+SQRT((0.258*CPM)**2+0.536*(1.0-CPM)*((1.0/R
        DU=DU/(0.268*(1.-CPM))
        XI=R/R2
        IF(XI.LE.1.)GO TO 50
        DU=0.
        GO TO 60
50      DU=((DX-XH)/(XN-XH))*DU*(1-XI**1.5)**2+
       3((XN-DX)/(XN-XH))*(1.0-(1.0-(1.0-XI)**1.5)**2)
        DU=DU*(1.0-1.0/CPM)
60      VINT=1.-DU
        GO TO 100
C
C       DX BELONGS TO REGION 3
C
20      R2=R22+(DX-XN)*DRDX3
        GO TO 70
C
C       DX BELONGS TO REGION 4
C
```



FIGURE 2-12. (Continued)

```
C
C       CALCULATE THE DEFICITS
C
        SUBROUTINE VELOC(K2,CPM,AH,RD1,R21,R22,R23,XN,XH
       1,DRDX1,DRDX3,DRDX4,CO,DX,DY,VEL,ADD)
        LOGICAL YA,YB,ZA
        DIMENSION CO(6),VEL(100),ADD(44)
        VEL(1)=1.
        Y=DY-0.945*RD1
        Z=0.135*RD1
        K5=1
10      DO 20 I=1,22
        R=SQRT(Y*Y+Z*Z)
        CALL DEF(R,VINT,RD1,R21,R22,R23,XN,XH,DRDX1,DRDX3
       2,DRDX4,CO,DX,CPM)
        K4=(1-K5)/2
        J=I+22*K4
        DU1=1.0-VINT
        R=SQRT(Y*Y+(Z+2.0*AH)**2)
        CALL DEF(R,VINT,RD1,R21,R22,R23,XN,XH,DRDX1,DRDX3
       3,DRDX4,CO,DX,CPM)
        DU2=1.-(VINT-DU1)
        ADD(J)=ADD(J)+DU2*VEL(K2)
        YA=I.LE.7.OR.(I.GE.15.AND.I.LE.19)
        YB=I.GE.8.AND.I.LE.13.OR.(I.EQ.21)
        ZA=I.EQ.8.OR.I.EQ.14.OR.I.EQ.20
        IF(YA) Y=Y+0.27*RD1
        IF(YB) Y=Y-0.27*RD1
        IF(I.EQ.20) Y=Y-0.54*RD1
        IF(ZA) Z=Z+0.27*RD1*K5
20      CONTINUE
        IF(K5.EQ.-1)GO TO 30
        Y=DY-0.945*RD1
        Z=-0.135*RD1
        K5=-1
        GO TO 10
30      RETURN
        END
```

FIGURE 2-12. (Continued)

```
10      R2=R23+(DX-XN-10.)*DROX4
        GO TO 70
70      DU=-0.258*CPM+SQRT((0.258*CPM)**2+0.536*(1.0-CPM)/(R2*R2))
        DU=DU*(1.-1./CPM)/(0.268*(1.0-CPM))
        IF(R.LE.R2)GO TO 80
        DU=0.
        GO TO 90
80      DU=DU*(1.-(R/R2)**1.5)**2
90      VINT=1.-DU
100     RETURN
        END



C
C       POWER CALCULATION
C
        SUBROUTINE POWER(K1,VEL,PRAT,ADD)
        DIMENSION VEL(100),PRAT(100),ADD(44)
        PRAT(K1)=0
        VEL(K1)=0
        DO 10 I=1,44
        PRAT(K1)=PRAT(K1)+((1.-ADD(I))**3)/44.
        VEL(K1)=VEL(K1)+(1.-ADD(I))/44.
10      CONTINUE
        RETURN
        END


C
C       AVERAGE
C
        SUBROUTINE AVER(N1,A,PRAT)
        DIMENSION PRAT(100)
        A=0
        DO 10 I=1,N1
        A=A+PRAT(I)
10      CONTINUE
        A=A/N1
        RETURN
        END
```

FIGURE 2-12. (Concluded)

Inputs are in the following order: first the array geometry is specified, second, the parameters describing the upstream meteorological conditions and the wind turbine height above the ground and its power coefficient are called for, and finally, the wind angles of interest are set.

Input is by means of cards and is in the following format:

Card 1: Title card; format 20A4
Card 2: N1; format I2 (number of wind turbines)
Card 3 to
Card N1 + 2: x, y; format 2F10.4 (wind turbine coordinates)
Card N1 + 3: $\alpha$ , m, H, $\alpha_e$; format 4F10.4
Card N1 + 4: $\theta_{start}$, $\theta_{final}$, $\Delta\theta$; format 3F10.4

In this scheme, both the x and y coordinates of the wind turbines in the array as well as the height of their centerlines above the ground, H, should be non-dimensionalized with respect to the rotor radius, $r_d$, before input to the program. Note!

Figure 2-13 is an example of the output of the computer program for a relatively simple array of four wind turbines, for a range in wind direction. The original wind turbine coordinates as well as the input meteorological parameters are printed at the top of the page. In addition, the various wake radii and wake growth rates are presented. For each wind direction, the coordinates (in the original system) are again shown for each wind turbine properly arranged with respect to the wind-oriented numbering system previously described. The individual power ratio for each wind turbine is shown as well as the average for the whole array.

Table 2-1 defines the symbols used in the FORTRAN program. Chapter 4 briefly discusses the utility of the present program and presents the reuslts of the program output for the cases of several selected arrays.

```
RUN NUMBER  1

THE  4 WINDMILL COORDINATES

      X          Y

   2.0000     2.0000
  -2.0000     2.0000
  -2.0000    -2.0000
   2.0000    -2.0000

INPUT VARIABLES

ALPHA=       .0500 CPM=      2.0000 AM=      2.0000 AMA=      1.0900
FI=    180.0000 FI2=    270.0000 DG=     10.0000

   XN= 12.84 RG=  1.22 R21=  1.41 R22=  1.62 R23=  2.69 DRDX1=   .05 DRDX3=   .11 DRDX4=   .10

*****************************************************************************************
      X          Y        P-RAT          WIND-DIRECTION  180.
   -2.0000    -2.0000     1.0000
    2.0000    -2.0000     1.0900
   -2.0000     2.0000      .1459
    2.0000     2.0000      .1459
                                        AVERAGED POWER RATIO FOR THE WHOLE ARRAY = .573

*****************************************************************************************
      X          Y        P-RAT          WIND-DIRECTION  190.
   -2.0000    -2.0000     1.0000
    2.0000    -2.0000     1.0000
   -2.0000     2.0000      .3914
    2.0000     2.0000      .3914
                                        AVERAGED POWER RATIO FOR THE WHOLE ARRAY = .696

*****************************************************************************************
      X          Y        P-RAT          WIND-DIRECTION  200.
   -2.0000    -2.0000     1.0000
    2.0000    -2.0000     1.0000
   -2.0000     2.0000      .7288
    2.0000     2.0000      .7283
                                        AVERAGED POWER RATIO FOR THE WHOLE ARRAY = .864

*****************************************************************************************
      X          Y        P-RAT          WIND-DIRECTION  210.
   -2.0000    -2.0000     1.0000
    2.0000    -2.0000     1.0000
   -2.0000     2.0000      .9630
    2.0000     2.0000      .7418
                                        AVERAGED POWER RATIO FOR THE WHOLE ARRAY = .926

*****************************************************************************************
      X          Y        P-RAT          WIND-DIRECTION  220.
   -2.0000    -2.0000     1.0000
    2.0000    -2.0000     1.0000
   -2.0000     2.0000     1.0000
    2.0000     2.0000      .3935
                                        AVERAGED POWER RATIO FOR THE WHOLE ARRAY = .826

*****************************************************************************************
      X          Y        P-RAT          WIND-DIRECTION  230.
   -2.0000    -2.0000     1.0000
   -2.0000     2.0000     1.0000
    2.0000    -2.0000     1.0000
    2.0000     2.0000      .3936
                                        AVERAGED POWER RATIO FOR THE WHOLE ARRAY = .826

*****************************************************************************************
      X          Y        P-RAT          WIND-DIRECTION  240.
   -2.0000    -2.0000     1.0000
   -2.0000     2.0000     1.0000
    2.0000    -2.0000      .9630
    2.0000     2.0000      .7419
                                        AVERAGED POWER RATIO FOR THE WHOLE ARRAY = .926

*****************************************************************************************
      X          Y        P-RAT          WIND-DIRECTION  250.
   -2.0000    -2.0000     1.0000
   -2.0000     2.0000     1.0000
    2.0000    -2.0000      .7287
    2.0000     2.0000      .7282
                                        AVERAGED POWER RATIO FOR THE WHOLE ARRAY = .864

*****************************************************************************************
      X          Y        P-RAT          WIND-DIRECTION  260.
   -2.0000    -2.0000     1.0000
   -2.0000     2.0000     1.0000
    2.0000    -2.0000      .3913
    2.0000     2.0000      .3913
                                        AVERAGED POWER RATIO FOR THE WHOLE ARRAY = .696

*****************************************************************************************
      X          Y        P-RAT          WIND-DIRECTION  270.
   -2.0000     2.0000     1.0000
   -2.0000    -2.0000     1.0000
    2.0000     2.0000      .1459
    2.0000    -2.0000      .1459
                                        AVERAGED POWER RATIO FOR THE WHOLE ARRAY = .573
```

FIGURE 2-13. Output example for 4-element array.

TABLE 2-1. Symbols used in FORTRAN program.

| Name | Type | Contains |
|---|---|---|
| ADD | Array (44) | The 44 registers used to sum the velocity deficits |
| AH | Real | Height of the hub |
| ALPHA | Real | $\alpha$ = ambient turbulence |
| AMA | Real | $\alpha_e/\alpha$, Turbulence ratio ~~$\alpha_e$ = alpha effective~~ |
| AVER | Subroutine | Subroutine to calculate the mean power ratio |
| CO | Array (6) | Constants calculated in subroutine CONST |
| CONST | Subroutine | Subroutine to calculate the wake geometry |
| COORD | Subroutine | Subroutine to rearrange the wind turbines |
| CPM | Real | m = initial velocity ratio |
| DEF | Subroutine | Subroutine used in VELOC to calculate the velocity deficits |
| DG | Subroutine | The difference in wind angle between two calculations |
| DRDX1 | Subroutine | dr/dx in initial and transition region |
| DRDX3 | Subroutine | dr/dx in region 3 |
| DRDX4 | Subroutine | dr/dx in region 4 |
| DX | Subroutine | $\Delta$ X between the wake producing and the receptor wind turbine |
| DY | Subroutine | $\Delta$ Y between the wake producing and the receptor wind turbine |
| FI | Subroutine | Angle of incoming wind |
| FI2 | Subroutine | The last wind angle to compute for |
| IFI | Integer | Integer used to calculate the direction of the incoming wind |
| K1 | Integer | Integer to keep track of the receptor wind turbine |
| K2 | Integer | Integer to keep track of the wake producing wind turbine |

TABLE 2-1. (Continued)

| Name | Type | Contains |
|---|---|---|
| K3 | Integer | Integer used to know when to stop increasing K2 |
| N1 | Integer | Number of wind turbines |
| N2 | Integer | Number of wind angles to do the calculations for |
| NR | Array (100) | Array used to keep track of the original geographic coordinates XG, YG |
| P | Real | Mean power ratio for the whole array |
| POWER | Subroutine | Subroutine to calculate the power ratio and mean velocity |
| PRAT | Array (100) | Power ratios calculated in subroutine POWER |
| R21 | Real | Wake radius at end of initial region |
| R22 | Real | Wake radius at end of transition region |
| R23 | Real | Wake radius at end of region 3 |
| RD1 | Real | Wind turbine disc radius after slipstream expansion |
| R0 | Real | Wind turbine disc radius before slipstream expansion |
| SORT | Subroutine | Subroutine to renumber the array |
| VELOC | Subroutine | Subroutine to calculate and add the velocity deficits |
| VEL | Array (100) | Mean velocities calculated in subroutine POWER |
| X | Array (100) | The x-coordinates in the wind-wise coordinate system |
| XG | Array (100) | The x-coordinates in the geographical coordinate system |
| XH | Real | Length of initial region |
| XN | Real | Length of initial and transition region |
| Y | Real | Used to calculate the velocity deficits in subroutine VELOC |
| Y | Array (100) | The y-coordinates in the wind-wise coordinate system |
| YG | Array (100) | The y-coordinates in the geographical coordinate system |
| Z | Real | Used to calculate the velocity deficits in subroutine VELOC |
| ZERO | Subroutine | Subroutine to reset storage array to zero |

# 3. FLUID MECHANICS

## 3.1 Wake Growth and Geometry

Earlier work in this program (Lissaman, 1977) presented the basic theory involved in determining the geometry and the flow in the wake behind a single wind turbine. There, it was pointed out that the wake constitutes a prescribed portion of the flow downstream of the turbine in which the momentum deficit is invariant. This momentum deficit represents the drag force imparted to the flow by the energy extraction disk operating at a given power setting, and is conserved at all downstream locations.

It is noted that the ground plane shear force will produce a small effect tending to change this momentum deficit downstream. In the case of no turbine disks this surface shear is exactly balanced by turbulent shear in the planetary boundary layer. Here we will assume that same effect occurs when the disk is present, thus the disk perturbation should be entirely represented by momentum deficit.

Thus, the flow properties in the wake are related to the operating conditions of the turbine itself. The conservation of momentum deficit in the downstream direction provides a relationship between the (decreasing) velocity decrement as the wake continues to increase in size due to turbulent growth.

Both of these latter factors (wake size and velocity) must be known in order to calculate the effects on available power to a downstream machine contained wholly or partially in the "degraded," or less energetic wake flow. In addition, the variation of velocity decrement over the cross-section of the wake is functionally related to the radius according to experimental profiles determined by Abramovitch (1963).

Thus, the wake can be visualized approximately as a conically diverging zone of velocity decrement behind the power extraction disk. The

velocity decrement is functionally related to the radius for all downstream locations, and its absolute magnitude decreases in the downstream direction. Sufficiently far downstream, the velocity decrement approaches zero, which is equivalent to saying that the wake flow returns to the free stream velocity.

The growth of the wake as the flow proceeds downstream is a result of the turbulent velocities in the vicinity of the wake edge. These turbulent velocities result from two main factors, mechanical turbulence caused by the extraction of energy from the flow by the turbine rotor, and the omnipresent, ambient turbulence contained in the free stream flow.

The mechanical turbulence is mainly a function of the shear which develops at the interface between the outer flow and the slower moving wake. It is most predominant in the initial portions of the wake where the shears are strongest and the wake radius is smallest. Farther downstream, the shear is less (the wake has speeded up and grown in size), and increased wake radius due to ambient turbulence further dilutes the effectiveness of the mechanical turbulence as a continuing wake increasing mechanism. Thus, in the downstream region, ambient turbulence dominates wake growth and mechanical turbulence can be entirely neglected. In the intermediate wake regions the combined effects of both mechanical and ambient turbulence are important to wake growth. Thus, the wake growth is not constant with downstream distance.

Figure 3-1 shows the important elements of the geometry of the wake behind the power extraction disk.

A short distance downstream of the disk, the flow is assumed to have changed from the uniform entering velocity profile of free stream speed to another uniform velocity profile of slower flow.

For a potential flow this would be represented by the well-known cylindrical vortex sheet and the associated slipstream expansion. In the real

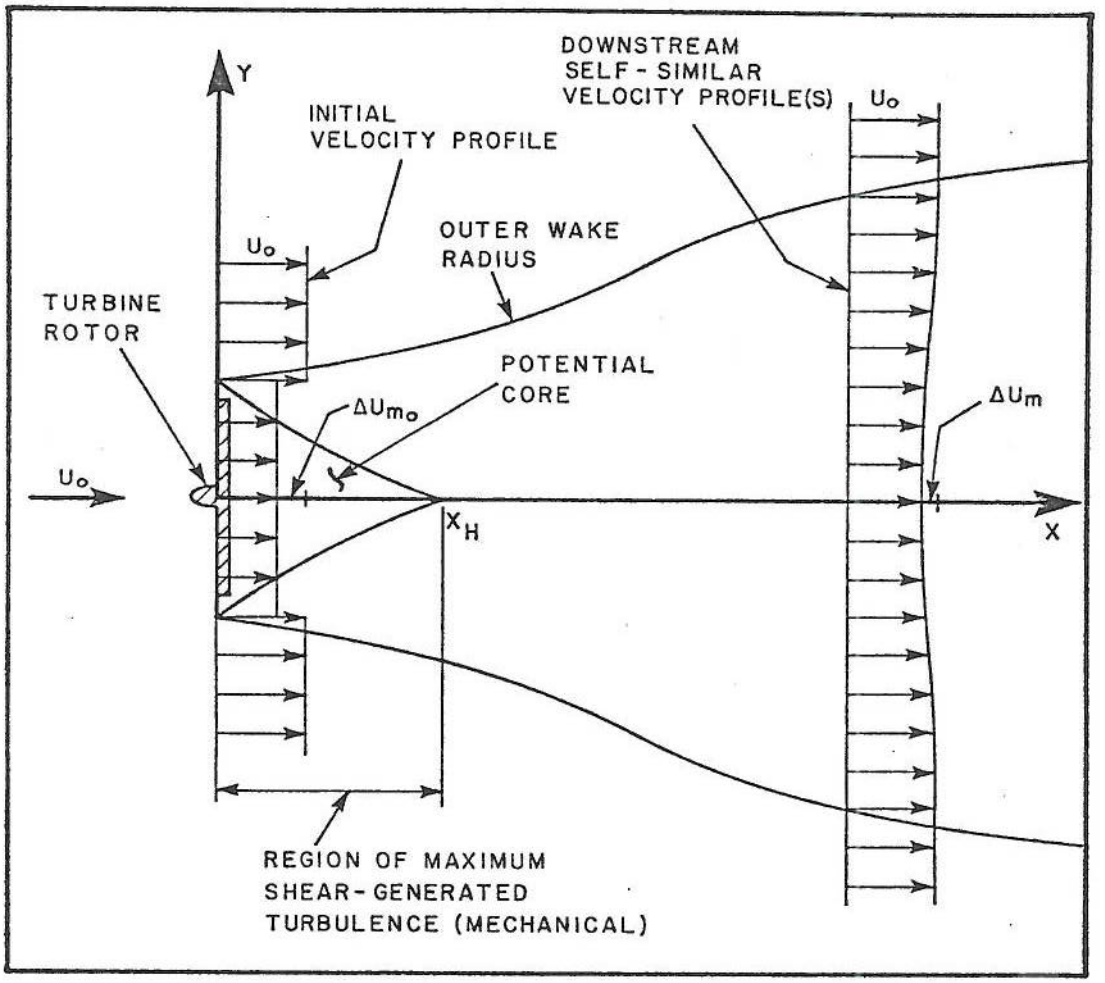


FIGURE 3-1. General wake geometry.

case it is this velocity gradient which initiates the development of the shear layer which causes the potential core to erode and the outer radius to increase. The difference in velocities is the initial velocity decrement and it is determined by equating the resulting momentum deficit to the total drag of the turbine as previously discussed.

As the flow proceeds downstream, the exterior flow mixes with and exerts shear forces on the slower moving wake fluid with the result that the entire wake flow begins to return to the free stream value.

By the time that the distance $X_H$ has been reached, the shear from the outer flow has completely eroded the potential core of uniform velocity.

An interesting problem occurs in modeling the combined effects of mechanical and ambient turbulence on development in this particular region since there is turbulent mixing both on the exterior circumference of the jet and on the interior where the potential core is being eroded. Now the standard approach (used in the main jet) is to determine the rate of wake growth due to mechanical terms and that due to ambient terms and combine by taking the square root of the sum of the squares. In this case this procedure can be applied to the outer turbulent periphery or the inner turbulent periphery. Models using both these assumptions were constructed and it was found that the differences were quite significant, the model based on the outer flow mixing giving wake growth rates about twice as large as the model based on erosion of the inner core. It was decided to use the latter model, on the grounds that this model does reflect the non-monotonic wake growth predicted and reported by Abramovitch for zero ambient turbulence. In the cited reference it is shown that during the core erosion stage the wake growth rate is somewhat less than the rate in later stages when the core is gone.

Thus the model we have used corresponds to that successfully used by Abramovitch for the zero ambient turbulence case. The cited reference computes the distance to full erosion of inner core by mechanical

turbulence; the present work computes the distance to full erosion of inner core by combined ambient and mechanical turbulence. Then in both cases the outer radius is uniquely determined by drag conservation.

A further operational reason for this choice was that the assumption of lower wake growth is usually conservative for performance calculations for simple arrays, since directly downwind units usually suffer the greatest energy flux loss.

At the downstream distance $X_N$, a radial velocity profile has established itself which is self-similar for all subsequent downstream locations.

This velocity profile, with its centerline scale velocity decrement, $\Delta U_m$, couples with the outer wake radius as prescribed by the conservation of momentum deficit.

The form of the relationship between outer wake radius and downstream distance as indicated by Figure 3-1 is in general a curve of varying slope as determined by the relative influences of the ambient and mechanical turbulence at different downstream locations.

A simplified form for wake radius was assumed for ease of computation. This form is presented and discussed in Section 2.3. Briefly, the wake was divided into various regions in which linear wake growth laws were assumed to obtain. A continuous function of wake radius vs. distance was obtained by appropriately matching the wake radius at the end points of each region. The definition and extent of the various wake regions as well as the wake growth laws and the functional forms of the velocity decrements in each is discussed in detail in Sections 2.3 and 2.4.

The power available to a downstream turbine contained in the wake of an upstream machine is determined by integrating the cube of the local wake velocity over the intercepted disk of the downstream turbine,

wherever it may be stationed in the wake. Dividing by the cube of the free stream velocity gives the power ratio compared to the case for full intercepted "free stream" power by the downwind machine. A pictorial representation of the geometry and the velocities mentioned above is given in Figure 3-2.

## 3.2 Interacting Wakes

The present study has refined the concepts developed earlier (Lissaman, 1977) and has added the feature of including the effects of multiple wind turbines, combined in an array. Thus, the power ratio for the array as a whole may be determined by individually considering each turbine in the array as a receptor (and all the others as generators) and then summing over the receptors. In order to do this, the velocities due to several upstream turbines oftentimes must be simultaneously considered as the entering velocity to a given receptor.

The total drag of a series of upstream turbines must be conserved across the entire resulting downstream wake structure. If the velocity decrements from each turbine are simply added in overlapping wake regions, then this deficit will be conserved providing the quadratic terms in the wake deficit are ignored. Thus this superposition is essentially a linearizing assumption. This is the method used here to account for the mutual wake effects of upstream machines.

For the situation where an upstream machine might itself be in the wake of a yet more upstream turbine, the following model was used.

In the same way that the power ratio was integrated across the disk of a receptor, the average entering velocity was also determined. All subsequent wake velocity decrements produced by this receptor-turned-generator, were scaled by the ratio of this average entering velocity to the free stream velocity. Thus, the free stream velocity was used for the scaling factor for the velocity decrements in the array in a manner similar

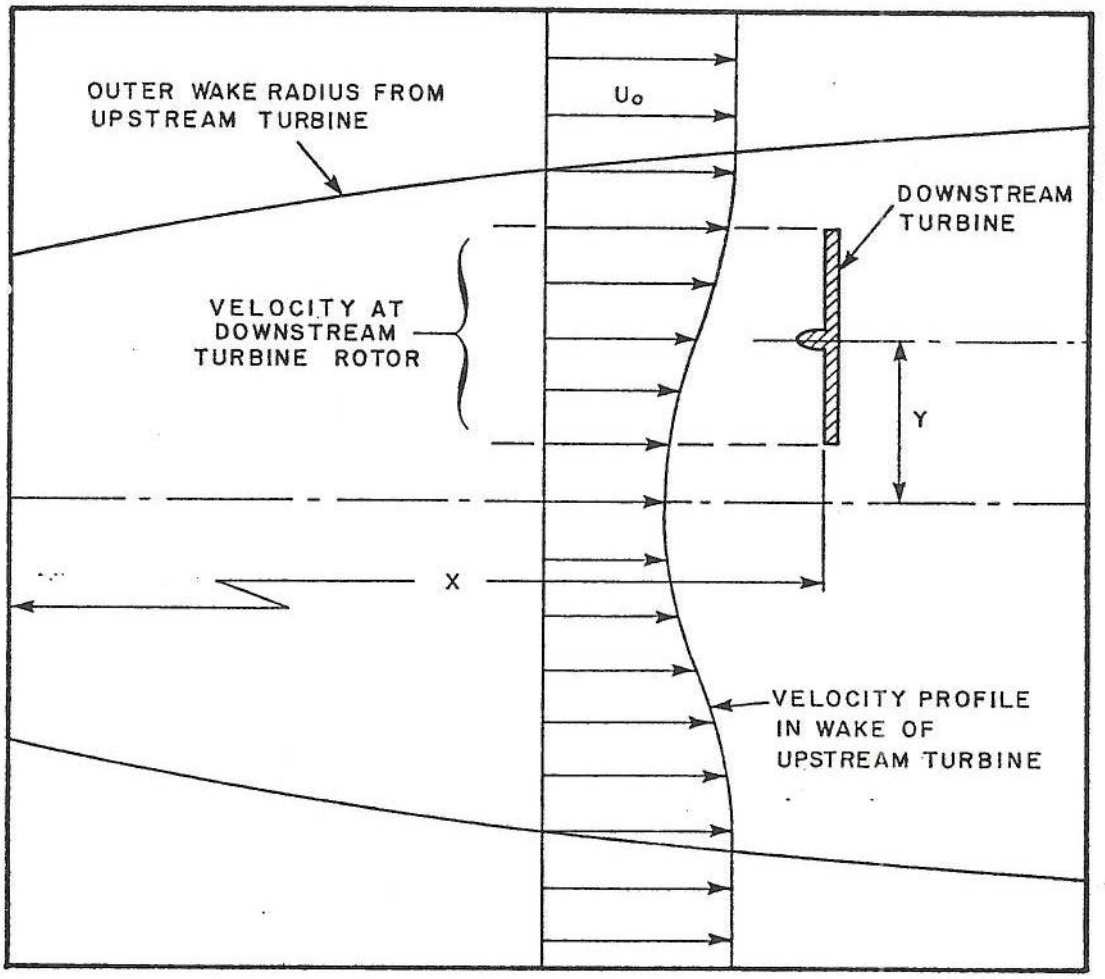


FIGURE 3-2. Velocity entering downstream windmill in the wake of an upstream unit.

to the way in which the cube of the free stream velocity is the scaling factor for the array power ratio.

### 3.3 Ground Plane

The effects of the ground plane are two-fold. First, it acts to slow the main flow due to friction in the well-understood fashion of the surface boundary layer. This is not included here since we consider only the perturbation due to the turbines. The effect of the entering velocity profile to the entire array is accounted for by appropriate selection of the array scaling velocity, $U_o$. Any effects of friction on the main flow within the dimensions of the array itself are expected to have negligible effects on power flux perturbation.

Secondly, the ground acts to reduce and eliminate the turbulent transport of momentum deficit and the mixing with the outer flow. Thus, wake velocities are smaller (decrement is larger) due to the presence of the ground.

This is modeled by the introduction of an image wake, spaced the same distance below the ground plane as the actual wake is above the ground. The velocity decrements in regions of wake overlap are added in the same manner as discussed in Section 3.2 for normal interacting wakes.

### 3.4 Initial Expansion Region

Due to axial pressure gradients in the region immediately downstream of the power extraction disk, the inviscid slipstream expands rapidly to a radius $r_o$, given by $r_o = r_d\sqrt{(m + 1)/2}$ , where $r_d$ is the actual disk radius. This expansion takes place in a downstream distance of about 3 $r_d$. However, during the actual expansion process, shear from the outer flow is continuously acting on the wake flow . From Figure 3-3, the combined effects of these two processes produces a "virtual" disk in the plane of the actual disk having a radius of $r_o$. It is from the edge of this virtual disk that

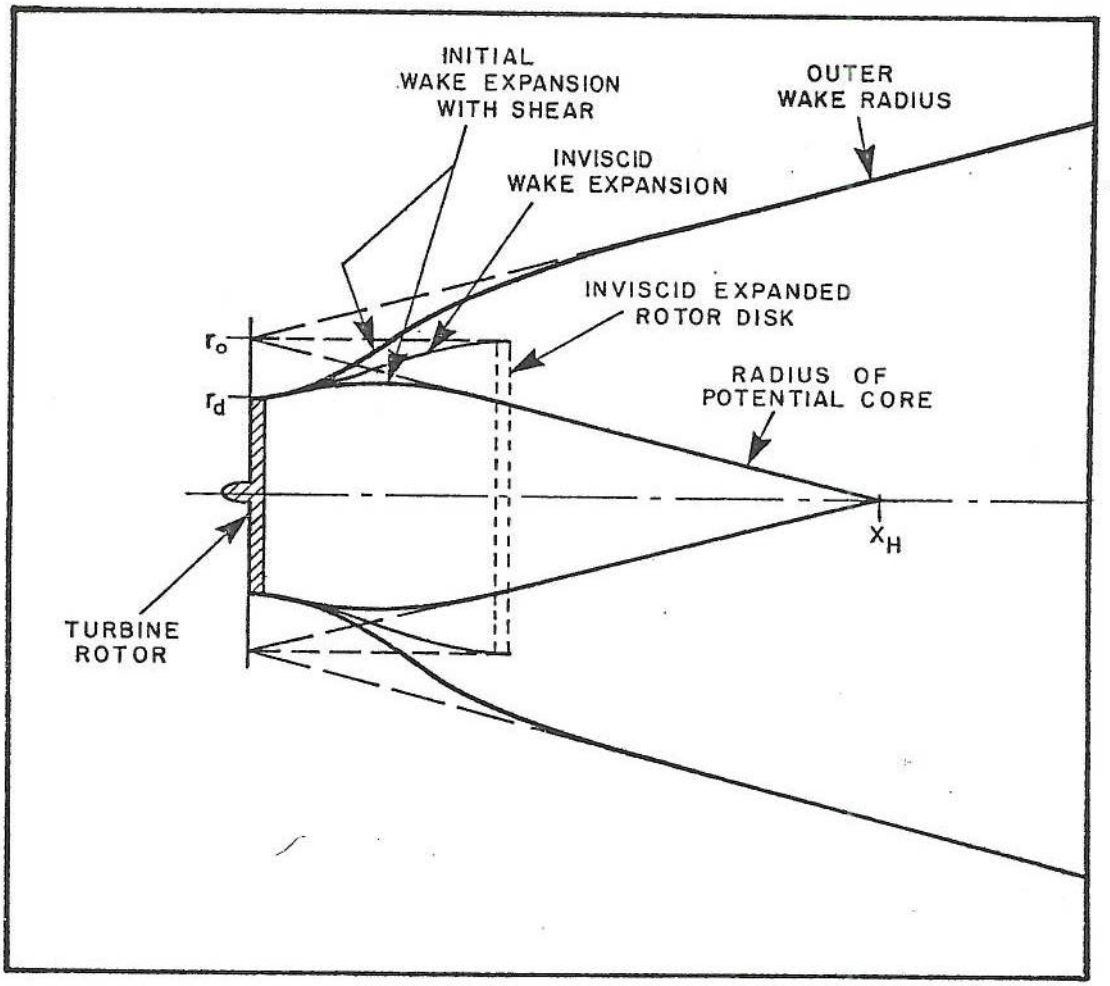


FIGURE 3-3. Initial wake expansion and shear layer.

all wake development proceeds. Figure 3-3 shows this geometry. The computer model was developed with the assumption that the initial wake growth from $r_d$ to $r_o$ occurred immediately at the origin of the downwind coordinate system and subsequent wake development proceeded therefrom. This is shown in Figure 3-3.

## 3.5 Transition Region Velocity Profile

The differences in the form between the velocity profile at the end of Region I and at the beginning of Region III are subtle, but real. There is either a discontinuous jump in wake radius if the centerline velocity decrements are matched, or the same jump in centerline $\Delta U_m$ if the wake radii are matched. This results from the requirement of drag conservation for both slightly dissimilar velocity profiles.

However, a transition region between the two different velocity regions in which the profile can smoothly change from one form to the other in a given downstream distance will also provide for the desired transition in wake radius.

This was accomplished in the program after the fashion shown in Figure 3-4.

On this figure, the velocity is desired at $r_1$ and X. The rule for combining the velocity decrements of the two known profiles, $f_1$ and $f_2$ is as follows:

$$\text{Let } \lambda = \frac{X - X_H}{X_N - X_H} \quad (0 \leq \lambda \leq 1).$$

Specify that:

$$\frac{r_1}{r_2} = \frac{r_{11}}{r_{21}} = \frac{r_{12}}{r_{22}}$$

($r_2, r_{21}, r_{22}$ are known).

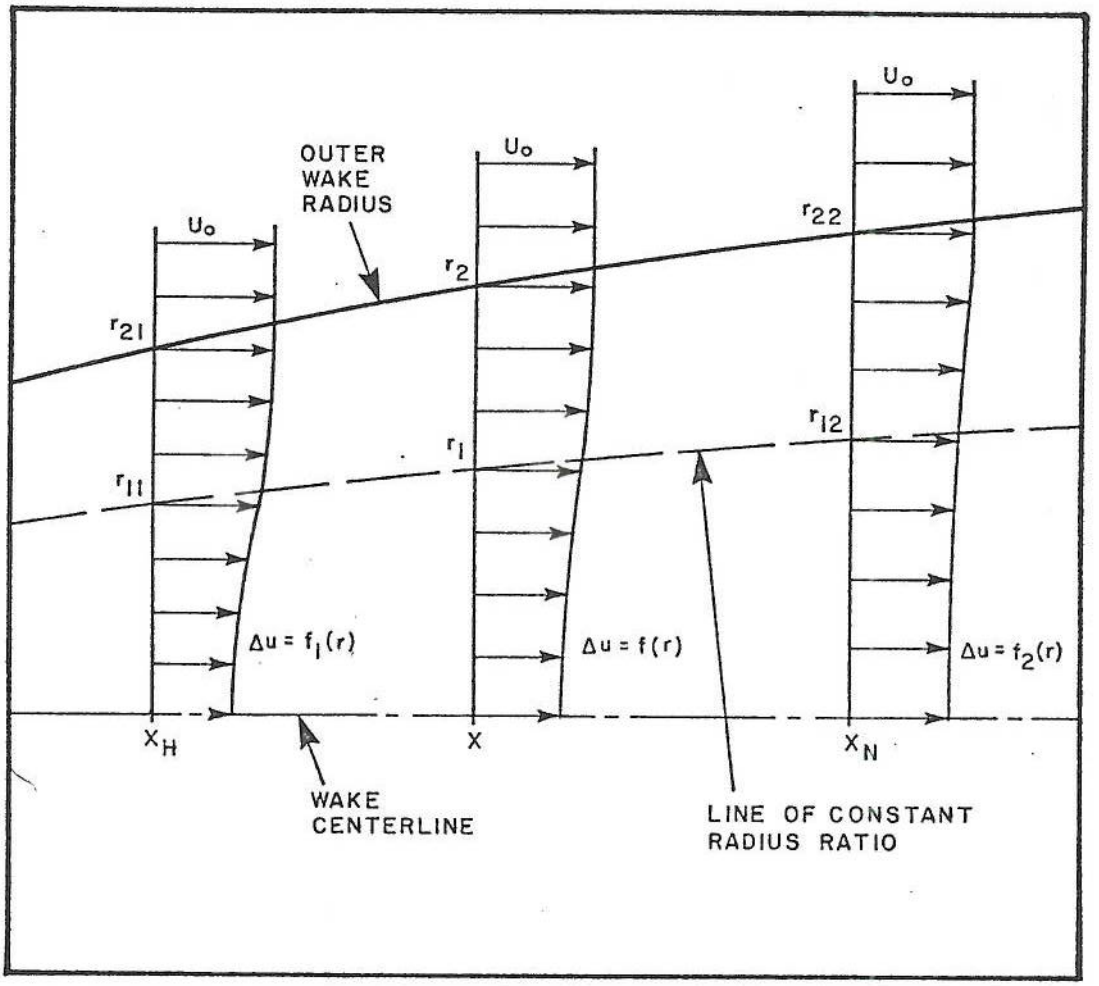


FIGURE 3-4. Velocity profiles in the transition region.

Then,

$$\Delta U = f(r_1) = (1 - \lambda)\, f_1 (r_{11}) + \lambda f_2 (r_{12})$$

gives the manner in which the velocity decrement is found at the point x, $r_1$ in the transition region.

## 3.6 Upstream Meteorology and Boundary Layer Effects

As has been discussed previously, an important parameter in wake development is $\alpha$, defined as $\alpha = q_t/U_o$ where $q_t$ is the effective rms ambient turbulence. This term couples with the turbulence mechanically generated by the wind turbine to give the effective turbulence controlling the rate of wake growth. For the computer model presented, $\alpha$ represents input data, that is, it must be selected for the given site, wind, and ambient conditions. Here we discuss some of the factors controlling $\alpha$. Ideally, one would determine $\alpha$ by field measurements of u', w', v', the rms turbulent fluctuations at turbine height at the site and then put $3q_t^2 = u'^2 + w'^2 + v'^2$.

An alternative technique is to use the Pasquill (1973) concepts of defining dispersion rate as a function of wind speed and cloud cover. According to this approach, given the wind speed, insolation, and cloud cover one can determine plume width $\sigma$ for various downwind distances X. For distances of less than a few kilometers this growth is approximately linear so that our $\alpha$ is defined by $\sigma = \alpha X$, where $\sigma$ and X are chosen appropriately.

Taking the version of the Pasquill curve given in Meteorology and Atomic Energy (Slade, 1968) we determine for neutral stability (Class D) that the vertical and lateral plume spreads $\sigma_z$, $\sigma_y$ are given as 5 and 8 m at 100 m and 34 and 70 m at 1 km. Now taking an effective $\sigma$ given by $2\sigma^2 = \sigma_z^2 + \sigma_y^2$ we obtain an $\alpha$ of .067 for 100 m and .055 for 1 km.

It should be noted that the Pasquill results are listed for a given ground roughness, described as "open level country." It is believed that this

corresponds to an effective ground roughness level $z_0$ of about 10 cm. For different values of $z_0$ adjustments to $\alpha$ must be made.

It is noted that methods for the estimation of $\alpha$ are not presented in this paper, where it is assumed that $\alpha$ is known.

### 3.7 Relationship between m and $C_P$

The analysis so far has used the parameter m as an indicator of the drag and power coefficients of the wind turbine. A simple relationship between these exists for an ideal actuator having a uniform axial interference factor, a. This can be expressed in the following equations:

$$m = 1/(1-a)$$

$$C_P = 4a\,(1 - a)^2$$

$$C_D = 4a\,(1 - a)$$

The above have been used in the present analysis. It is noted that m = 3 corresponds to maximum power extraction.

For a turbine operating under non-ideal conditions or with significant viscous losses we would expect to be given $C_D$ and $C_P$ as functions of the tip speed ratio. Thus one can write $C_P$ as a function of $C_D$. Thus the procedure here would be to specify $C_D$ and hence m by the previous equation and then to determine the appropriate $C_P$ for the real turbine.

It is noted that the analysis of this entire report does not depend upon any specific $C_P$ assumption. This is because drag conservation is the basic invariant, and the result is given in the generalized form of the relative energy flux through all the turbines. Thus any modeling of real $C_P$ effects can be made independently to the present analysis and will not affect the results.

# 4. EXERCISE OF COMPUTER MODEL

## 4.1 General

During the development of the computer model, the output of the program was continuously compared with the fluid mechanical assumptions involved in the physical formulation of the wake geometry. This was done using the output of the Hewlett Packard computer routine since this was the machine on which the development of the model was accomplished.

After the program was in a satisfactory form which incorporated all of the desired features mentioned in the earlier sections, it was transcribed to FORTRAN and the output was checked against the results of the Hewlett Packard version for several selected test cases. For all, the correspondence between the two versions of the program was identical, thus validating the accuracy of the transcription.

This section presents the results of the program for several representative array geometries. The input parameters to the program (ambient turbulence wind turbine operating conditions and turbine height) were identical for all cases and are given below. The parameters used for the examples here are quite representative of conditions that might be encountered for a real wind turbine array, representing a moderate wind (> 2 m/sec) blowing over flat grassland ($z_0$ = 10 cm) in a neutral stability atmosphere.

## 4.2 Centerline Power Ratio for Simple Geometry

The first task was to demonstrate the ability of the program to calculate the power ratio for the simple case of a wind turbine in the wake directly behind an upstream machine. The results of this investigation are presented in Figure 4-1.

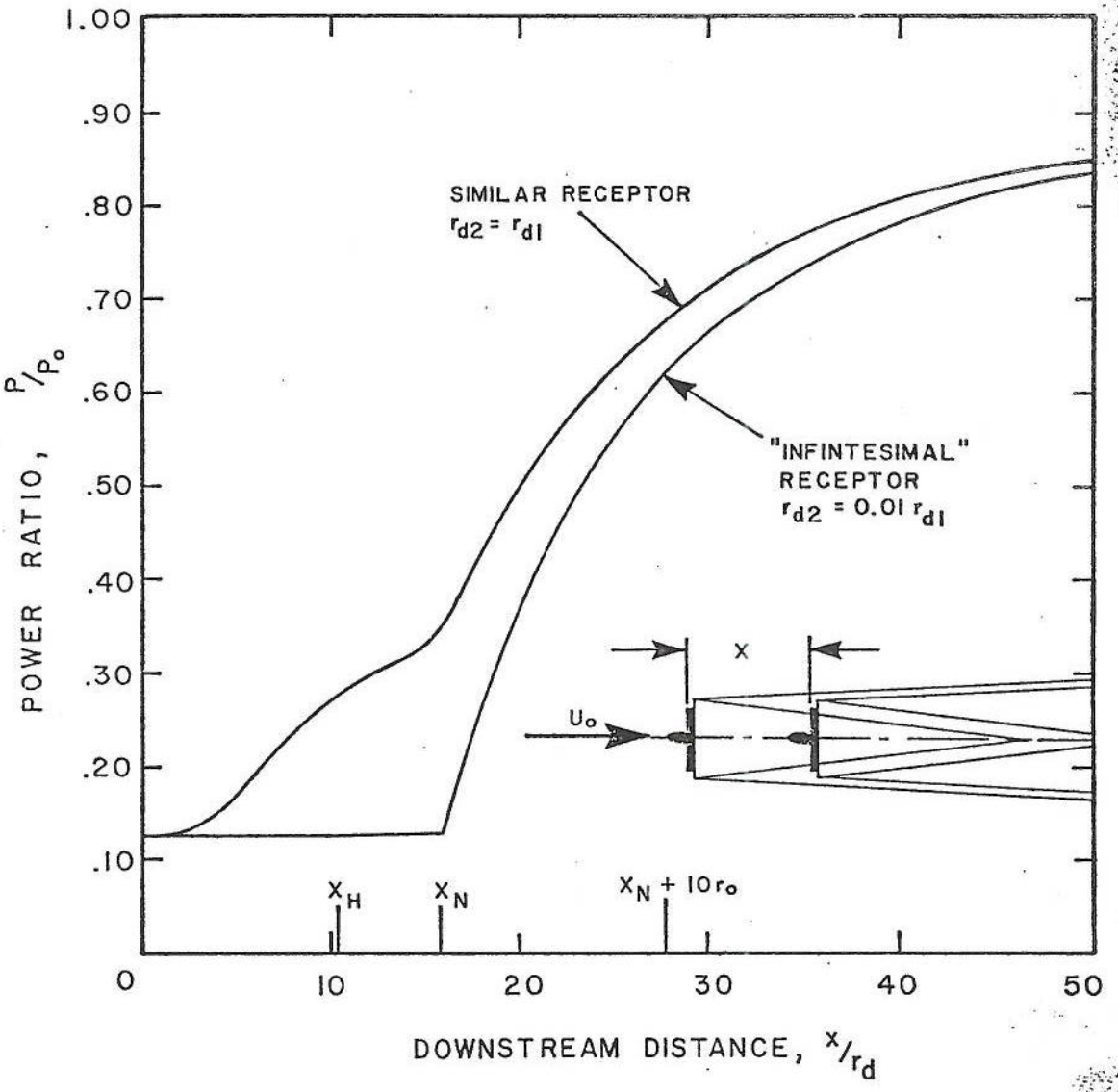


FIGURE 4-1. Centerline power ratio behind a wind turbine.

Here, two different cases are shown, that for a downwind machine identical in size to the upwind one, and that for a receptor which was very small compared to the generator. This latter case could only be run using the Hewlett Packard program since this included variable turbine disk size as an input. The FORTRAN version tacitly assumes an array in which all turbines are of the same diameter, and variable disk diameter is not an option for input.

For the case of the "infinitesimal" receptor, the power ratio assumes the proper value of $P/P_0 = 0.125$ directly behind the power extraction disk of the upstream machine for the value of $m = 2.0$ which was used for this example. This power ratio remains constant (as it should) in the potential core until $X = X_H$. At this point the power ratio increases slightly (in the transition region) until $X = X_N$ is reached. Then the power ratio begins to increase abruptly to the value of 1.0 for further increase in downstream distance.

The case for the similar receptor is somewhat similar. Due to slipstream expansion, the disk of the receptor is entirely within the potential core of the upstream machine when the former is immediately behind the latter. Thus, its power ratio is also $P/P_0 = 0.125$ for this position. Likewise, for far downstream distances when the effects of the momentum deficit of the wake are extremely diluted, the power ratio also asymptotically approaches the free stream value of $P/P_0 = 1.0$. Due to the finite size of the receptor, intermediate downstream positions result in varying effects of the interception of the velocity profile in the wake of the upstream turbine, and this is reflected in the total, integrated power ratio, as shown in Figure 4-1.

The power ratio does not immediately increase from 0.125 as the downstream distance is increased from zero. This is due to the fact that slipstream expansion results in a potential core of uniformly retarded flow larger than the disk of the wind turbine itself (for the case of $m = 2.0$ chosen here, $r_o = 1.22\ r_d$). Thus, some downstream distance must be reached by the

receptor before its edges reach the edge of the potential core, and it starts to experience the faster flow in the shear layer. However, beyond this point, the potential core reduces beyond the diameter of the receptor with a resultant increase in power ratio. At the end of the potential core region ($X = X_H$) the receptor is entirely in the shear flow, but the velocity does not change much over the downstream distance in the transition region ($X_H \leq X \leq X_N$). This is also shown by a more gradual increase in the power ratio in this region. At the end of the transition region (the beginning of the far wake), shear near the centerline is much reduced, and the power ratio more closely approaches the case of the "infinitesimal" receptor.

## 4.3 Complex Array Geometries

Figures 4-2 through 4-10 present the results of the power characteristics for five different arrays, the first two selected by AeroVironment as test cases, and the last three by the sponsor as potential siting cases.

The results are presented as average array power (free stream power ratio = 1.0) as a function of wind angle. No attempt was made to analyze these results in detail except to note that the maximum and minimum points occurred at wind angles consistent with the geometries involved.

The results are quite useful. They may be used directly to compare the virtues of one array geometry with those of another. For a given array, they quickly show the optimum wind angle for maximum power extraction. Also, for a range in wind angle, they may be multiplied by the temporal variation in that angle (for constant wind velocity) and then integrated to give a time average power for the array for the wind angle variation imposed. A more complicated integration could also incorporate the effects of varying wind speed or the effects of a wind vector with an assigned probability function for speed and direction.

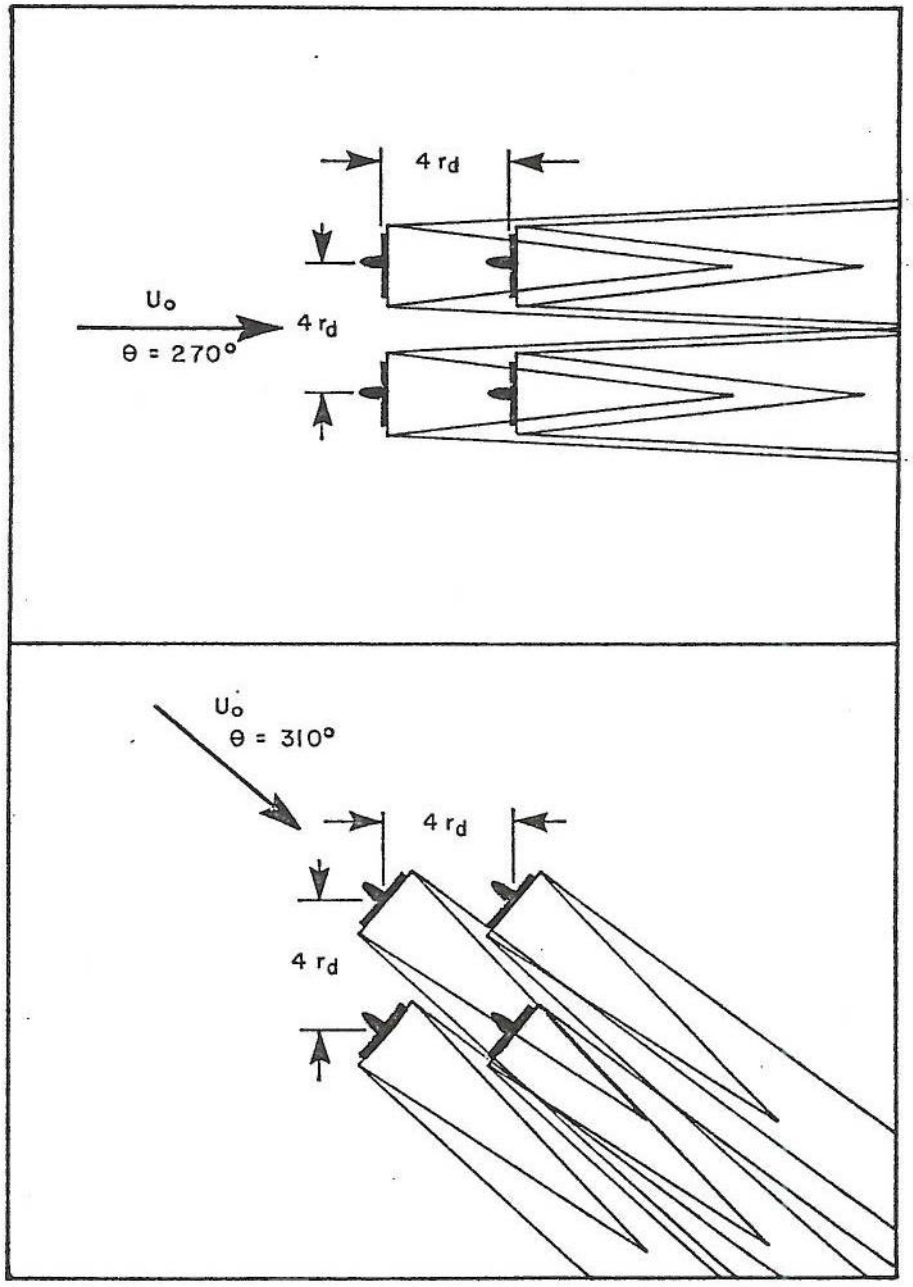


FIGURE 4-2. Square array of four wind turbines showing effects of wind direction.

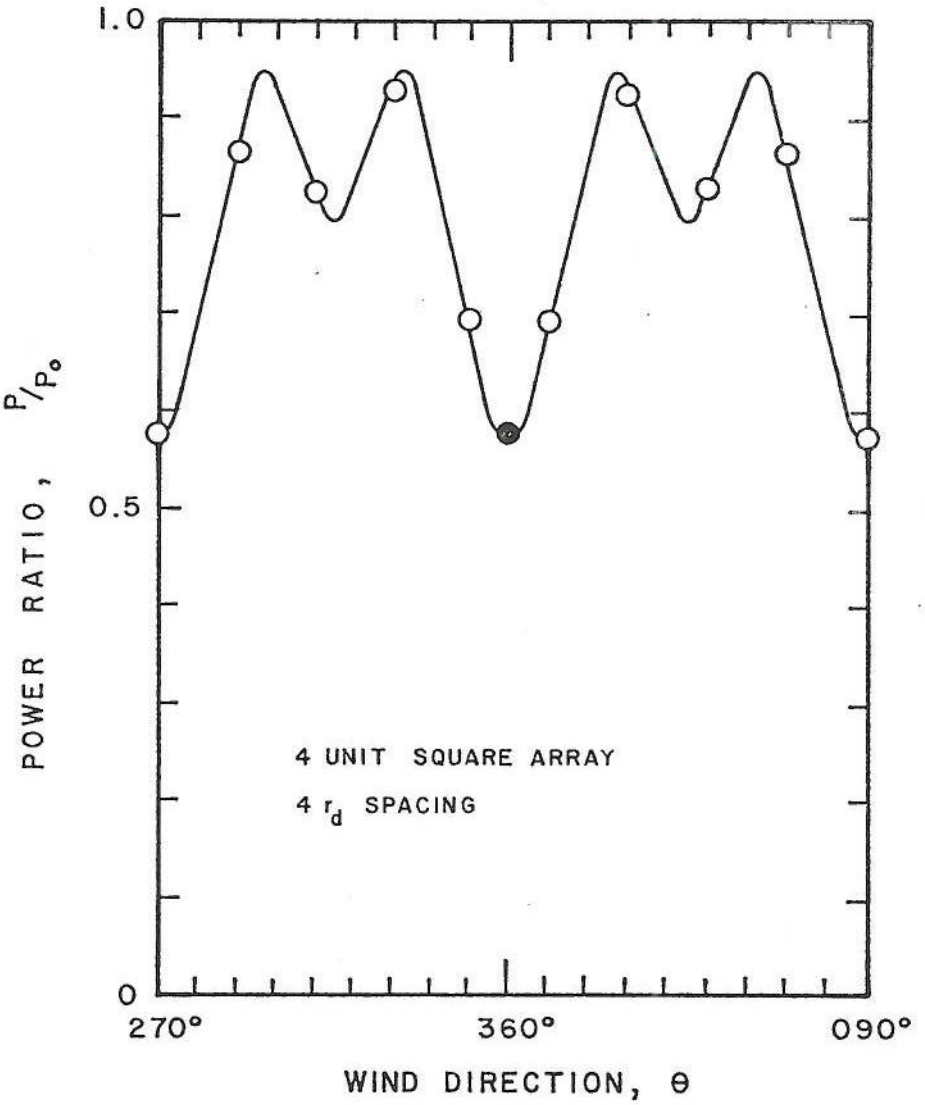


FIGURE 4-3. Power ratio for square array as a function of wind direction.

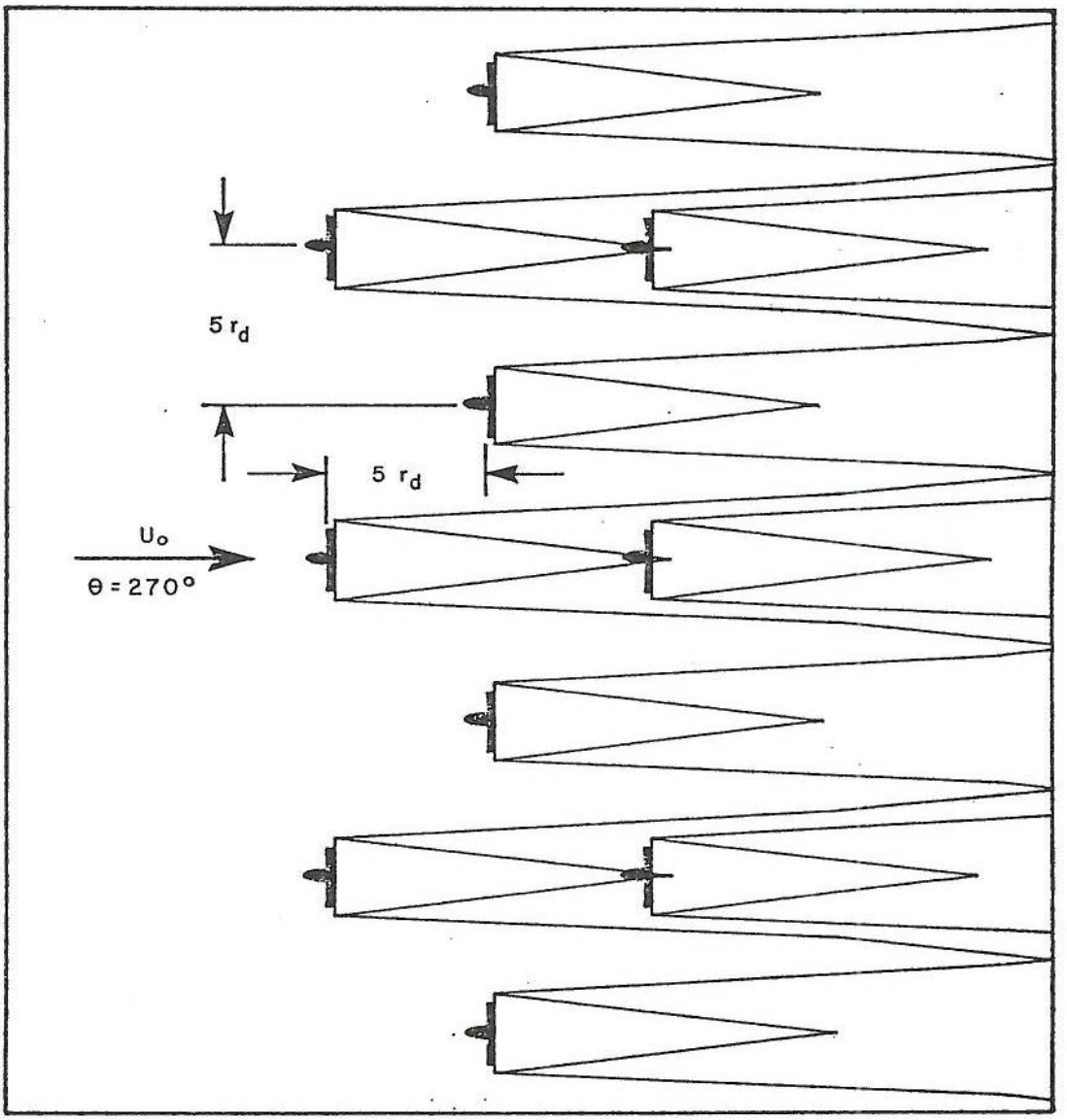


FIGURE 4-4. Staggered, three row array of 10 wind turbines.

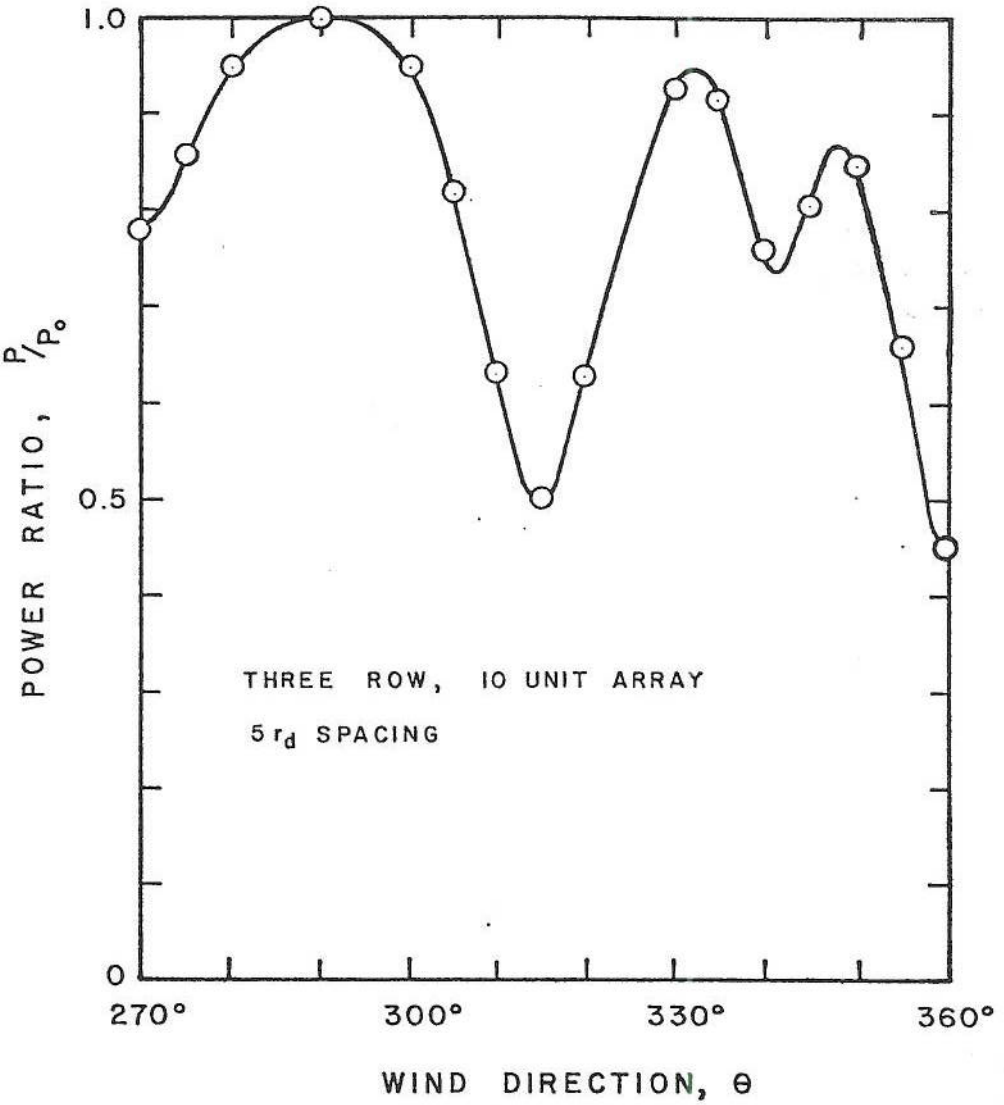


FIGURE 4-5. Power ratio for the staggered three row array as a function of wind direction.

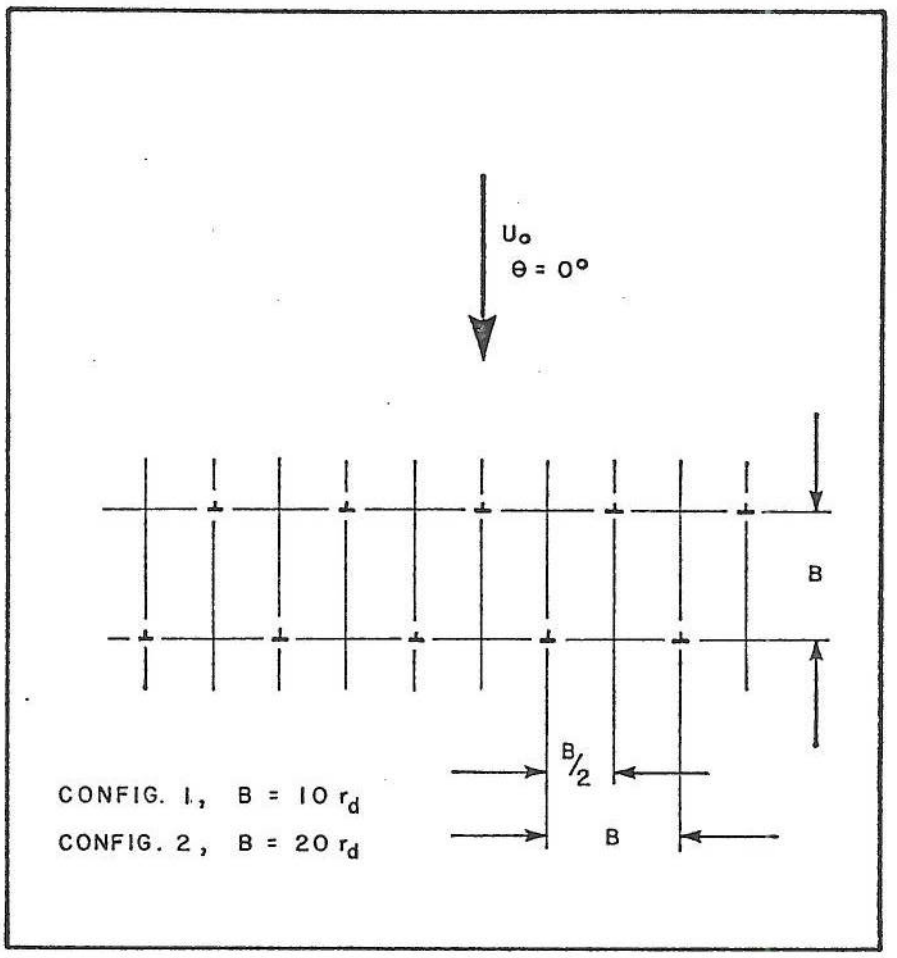


FIGURE 4-6. Two row rectangular array of ten wind turbines of two different configurations.

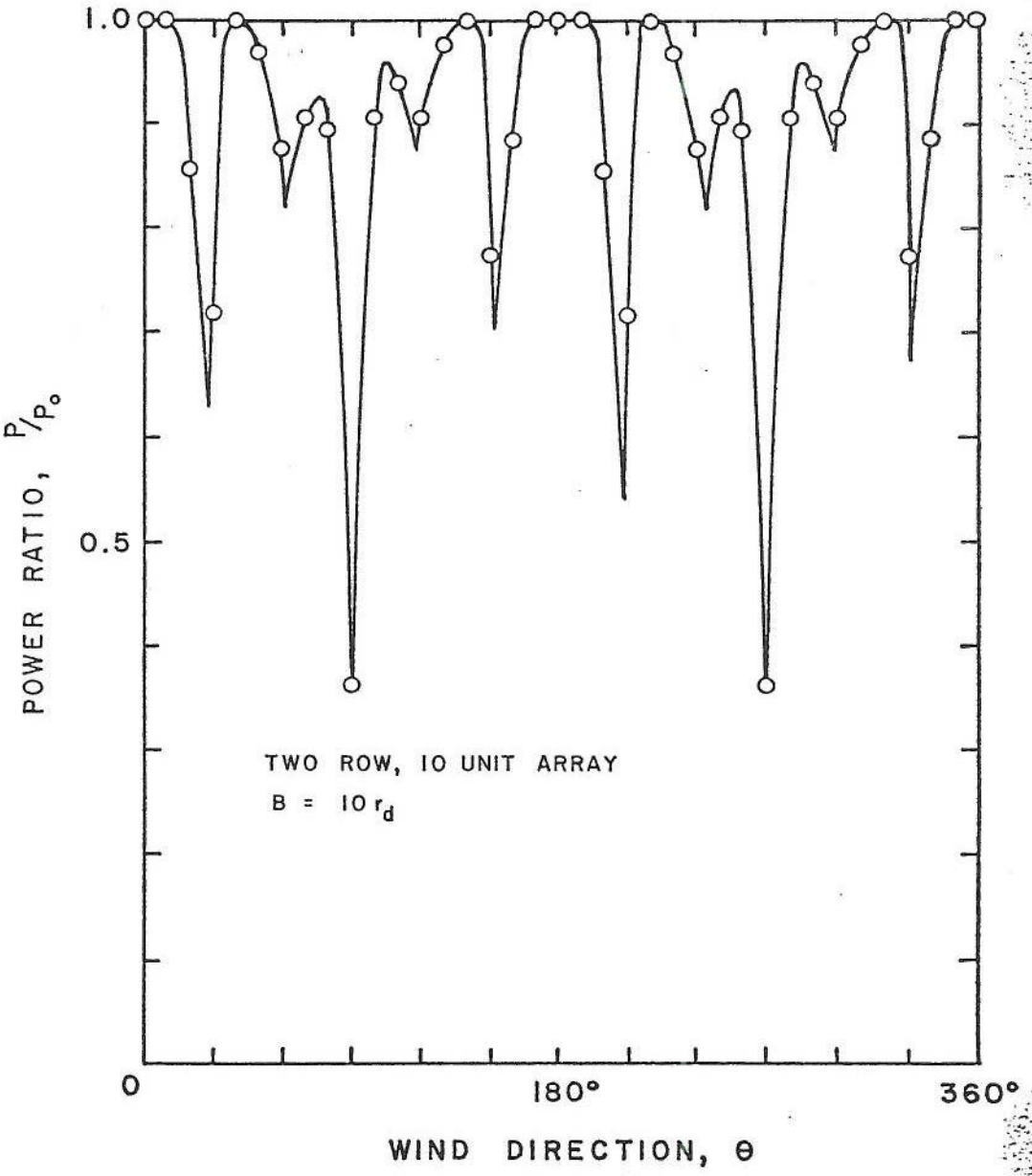


FIGURE 4-7. Power ratio for the two row, 10 turbine array (configuration 1), as a function of wind direction.

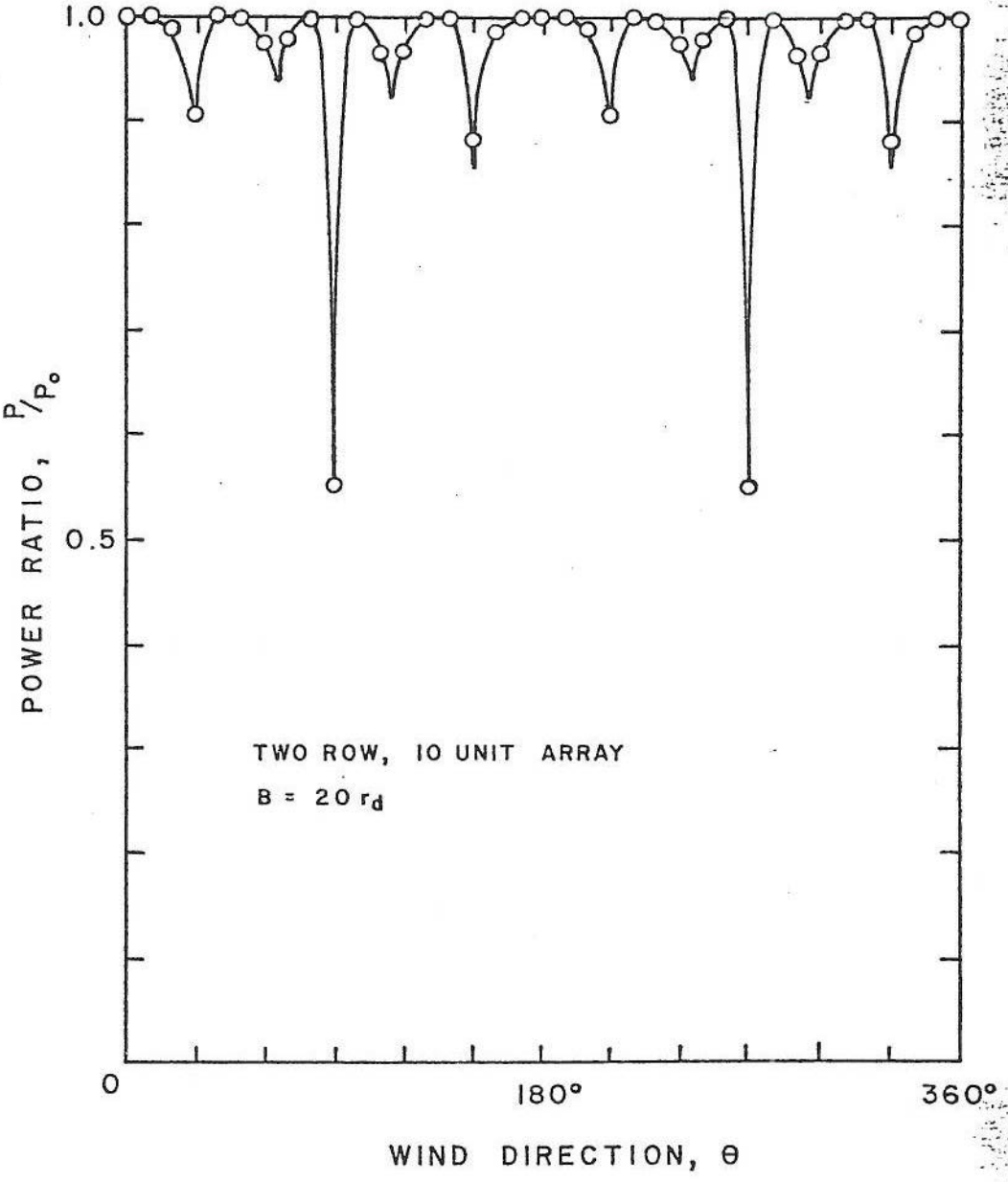


FIGURE 4-8. Power ratio for the two row, 10 turbine array (configuration 2) as a function of wind direction.

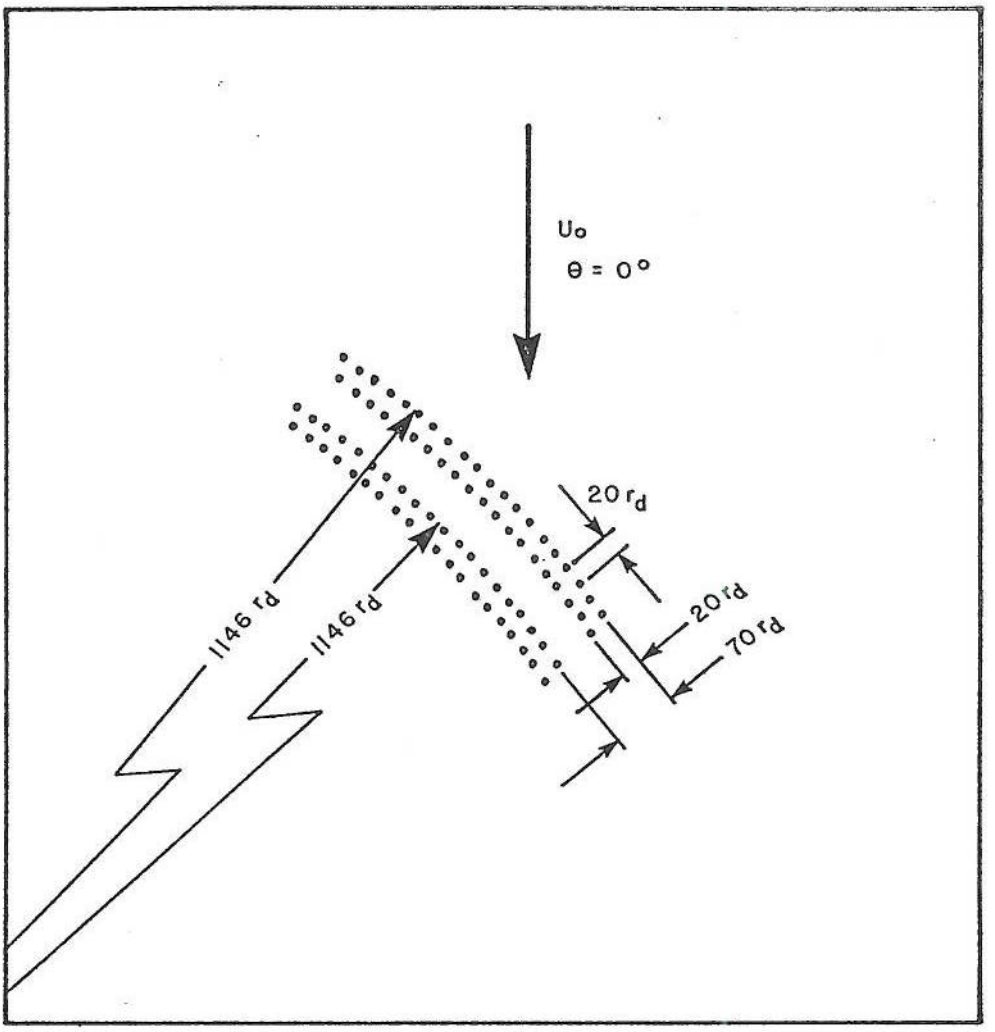


FIGURE 4-9. Curved, four row array of 80 wind turbines.

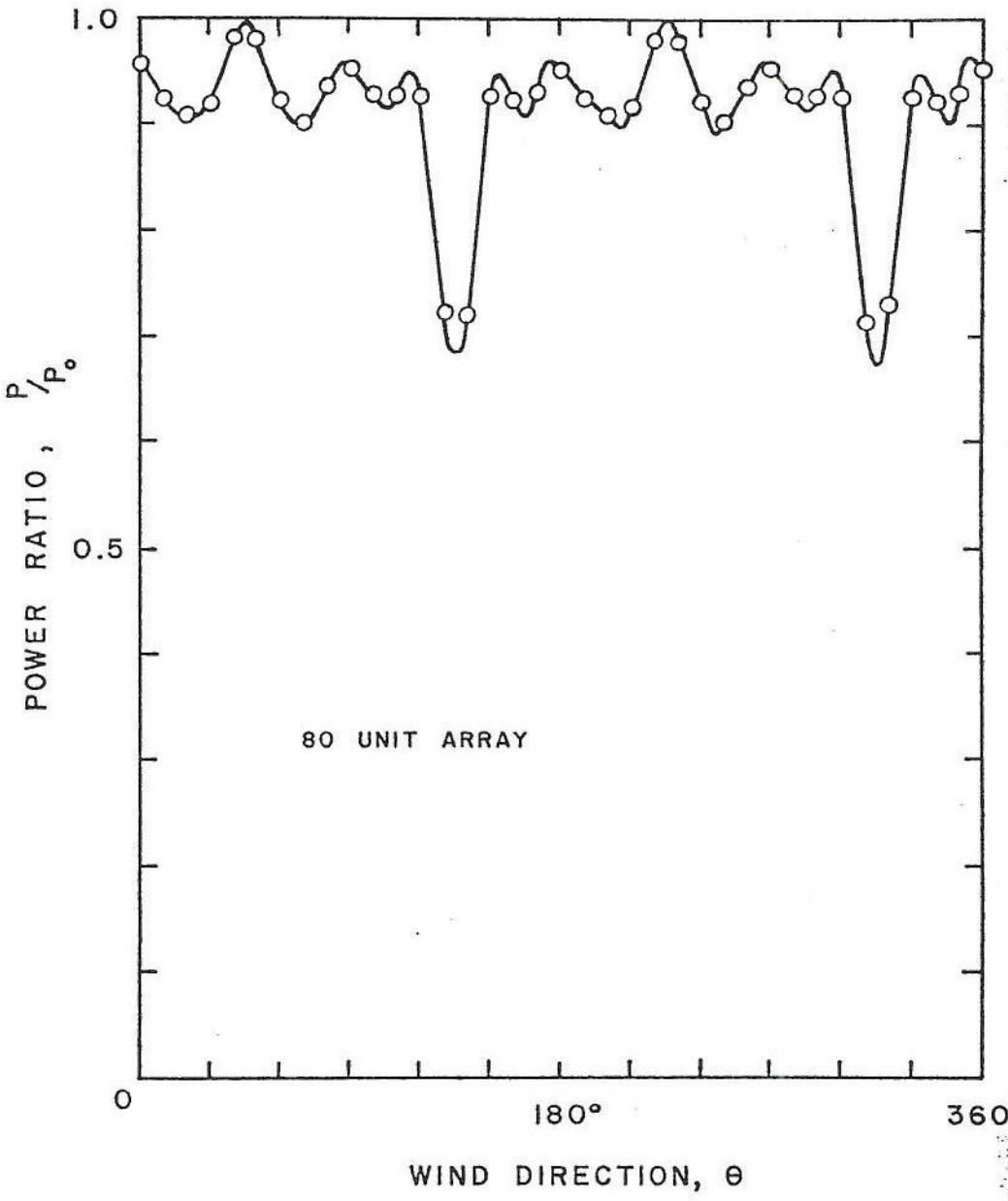


FIGURE 4-10. Power ratio for the 80 wind turbine array as a function of wind direction.

# 5. RECOMMENDATION FOR FURTHER WORK

## 5.1 General

The form in which the present computer model exists deals exclusively with the geometrical interaction of wind turbine wakes in arrays situated in flat and level terrain for which all of the turbines operate at constant local power coefficient. The results to date indicate that these wake interactions with other turbines in the array can have dramatic effects on the power available to them and to the array as a whole.

The present model deals with the major aspects of the problem and forms a valuable framework to investigate the effects of array geometry for many purposes related to the technical and economic effectiveness of wind turbine arrays. The computer code is written in such a way that the physical effects of various parameters and constants can readily be perceived and has the flexibility that these terms can be varied to reflect improved physical knowledge.

Thus it appears that all major influences are incorporated with functionally correct mathematics, and the program will converge properly to all limiting cases.

Evidently the model in its present form should be extensively exercised, and its results carefully assessed.

There are, however, three obvious areas in which further work could be profitably conducted. These are

1) Testing of the model against actual results obtained in field and wind tunnel experiments.

2) Improving the fluid mechanics and meteorology incorporated in the model by more complex representation of the flow field.

3) Improving and augmenting the computer program by incorporating additional subroutines and refinements.

Recommended work in these areas is discussed below.

## 5.2 Correlation with Test Results

Evidently the assumptions of wake growth and profile must be tested against good experimental data. The existing model will provide a foundation to design a number of basic tests. It appears that the most critical model assumption relates to the wake growth under combined mechanical and ambient turbulence. This important topic merits both theoretical and experimental study. Thus it is imperative that the testing include an airstream with a significant turbulence level. This will occur naturally in the field but in wind tunnels an atmospheric type turbulence structure must be created. A further important test concerns the characteristics of the wake of a wind turbine operating itself in the wake of an upstream unit. This feature may not be strongly dependent on ambient turbulence and could thus effectively be done in a wind tunnel with the associated freedom for extensive geometrical turbine placement changes.

## 5.3 Improved Fluid Mechanical Modeling

The present model has been developed for a uniform entering velocity profile. This is an approximation to the actual situation, where the planetary boundary layer produces a vertical shear gradient. The assumption of the present model is that using the wind speed at the turbine axis (or center of swept area for vertical axis machines) will be a satisfactory approximation for the non-uniform wind field. For example, for a circular disk with a linear vertical speed variation the error is about $.2\,(\Delta V/\overline{V})^2$ where $\Delta V$ is the total speed change from top to bottom of the disk and $\overline{V}$ the speed at the disk center. The distortions in the resulting wake geometry for a more complex profile in the model are quite complex and the fluid mechanics are difficult to represent mathematically for arbitrary array configurations.

However, since the ultimate goal of the computer program is the prediction of total array power and not the intimate flow details within the array, it is possible to approximate a boundary layer flow by a uniform flow for the purposes here by specifying a proper scale velocity.

This scale velocity will represent the average power available to the array in the boundary layer flow and will be a function of the geometry of the boundary layer in relationship to the size (height) of the wind turbines thus defining $\Delta V/\bar{V}$. The boundary layer geometry can be specified in terms of the wind speed measured at some reference height and the friction at the surface which is a function of the ground roughness.

Thus, an algorithm for the computer program can be specified which will intrinsically incorporate all of these factors. Total array power can thus be properly scaled to reflect the influence of the boundary layer.

It is noted that the effects of tower wake have not been incorporated into the fluid mechanics. Although these are knownto be significant to the rotor of the tower itself, it is believed that the effect on neighboring rotors would not be large. However, this aspect certainly merits examination.

A most important aspect of the fluid mechanics requiring further theoretical study is the problem of how the wake grows under combined ambient and mechanical turbulence. Some simple, but rational, assumptions have been used in the present model. These require validation. In particular, as has been noted in a previous section (3.1), ambiguities arise for the initial region, where there is turbulent entrainment from both outer and inner flow. The difference in general wake growth between assuming the process is controlled by inner or outer mixing is quite significant. Evidently more theoretical work would be very important here.

## 5.4 Improved Meteorological Modeling

For a proper exercise of the model it is evident that reliable inputs for the incoming natural wind speed and turbulence profiles are required. As is

well known these are functions of the roughness of the upstream fetch, the wind speed itself and the stability of the atmospheric boundary layer. Much experimental and theoretical data exists on this, particularly for the mean wind speed, although there is less known about the turbulence levels. It is believed that good models can be developed for this, at least for level terrain. For the complex terrain situation there is less reliable data, but the effects of flow channeling between ridges, and the speed-up factor associated with the crests of hills and ridges is certainly important since these constitute potentially attractive wind turbine sites.

## 5.5 Augmentation of the Computer Coding

Evidently before the program is augmented, analysis should be conducted to determine if it can be simplified in any fashion. The current code is believed to contain sufficient complexity to rationally handle all the important aspects. However, it may be that the four region wake model (or any other aspect of the code) is unnecessarily complex. Insights to this can be obtained by exercising the model for a number of special cases and conducting a sensitivity analysis of the different steps in the program. It is a matter of interest that this is seldom done on a satisfactorily functioning program with the end result that as the code is extended with a number of necessary refinements the program becomes excessively unwieldy and expensive to run.

Independent of the streamlining of the program described above, there are a number of obvious refinements which would add to the automation of the present program.

Evidently an improved meteorological model could be incorporated as a subprogram. Such a model would define wind and turbulence profiles for given wind speed, fetch roughness and insolation and could be designed to incorporate different approach fetches for wind from different directions at a given site.

A further useful subroutine would be one incorporating the actual engineering performance characteristics of the turbine systems including such real machine features as non-ideal drag and power coefficients as well as cut-in/cut-out speeds of the machines and their control characteristics.

With such meteorological and machine characteristics it would be possible to exercise the model with a probabilistic wind vector input and obtain monthly or annual power characteristics of a site along with means and expected variances of these characteristics.

## 6. REFERENCES


Abramovitch, G.N. (1963): The theory of turbulent jets. MIT Press.

Lissaman, P.B.S. (1977): Energy effectiveness of arrays of wind energy collection systems. AeroVironment Inc. Report AV R 6110.

Pasquill, F. (1974): Atmospheric diffusion. 2nd Ed. John Wiley and Sons.

Slade, D.H., ed. (1968): Meteorology and atomic energy. U.S. Atomic Energy Commission TID-24190.

# APPENDIX

## Determination of Effective Growth Rate in Region III

$$r_2/r_0 = [(1-m)(0.134\ \Delta\bar{U}m^2 + 0.258\ m\ \Delta\bar{U}m/1-m)]^{-1/2} \qquad (D)$$

From initial conditions of $r_2$, $\Delta\bar{U}m$ at the start of Stage III, equations (A) (B) (C) (D) were integrated numerically to determine $r_2$ at $\Delta X = 10\ r_0$. This involved assuming an increase in radius $\Delta r$, determining the mean values of $\Delta\bar{U}m$ over this range from (D), then using (A) (B) (C) to determine the mean combined growth rate from which the associated X distance is determined, and iterating this process until $\Delta X > 10 r_0$. Finally the effective growth rate $\alpha_e$ is determined for $\Delta X = 10\ r_0$.

From the numerical calculations it was noted that in all cases of $\alpha > 0.05$, the effective growth parameter $\alpha_e$ is only marginally different from $\alpha$, thus it is justified to assume the growth in this region is uniform, of rate proportional to $\alpha_e$.